DEVELOPMENT OF A LABEL-FREE DETECTION TECHNIQUE FOR HUMAN INFECTIOUS VIRUS BY RAMAN SPECTROSCOPY

DEVELOPMENT OF A LABEL-FREE DETECTION TECHNIQUE FOR HUMAN INFECTIOUS VIRUS BY RAMAN SPECTROSCOPY

A Thesis for the Degree

of

Doctor of Science

Submitted to

Graduate School of Science and Technology

Kwansei Gakuin University

By

Moor Kamila (67012703)

in January 2019

Table of contents

ABSTRACT

A patient-free real-time detection technique for human infectious virus would open a new era for virologists and be useful in the bio-environmental field as well as the medical field. Raman spectroscopy has significant potential for the analysis of viral materials in biological samples. Analysis of human infectious virus is often carried out using several types of cultured cells to incubate the virus. As it takes 5-10 days to obtain results because several days are required for incubation of the virus, the conventional methods are not useful to prevent the pandemic of a viral disease. In the present study, I used Raman analysis to identify a virus infection in live cells. The Raman technique is relatively safe for biological samples, such as live cells, because it is based on light scattering and does not directly contact the sample. The Raman spectrum contains information of molecular structures and conformations of the chemical species in the cell. The aim of this study was to develop the technique for the analysis of human infectious virus that does not require a patient and has a very quick response time. I have utilized recombinant adenovirus and human embryonic kidney (HEK) 293 cells as the model of cultured human cells and infecting virus to study how Raman spectroscopy was able to detect the infection. The developed technique was able to monitor the molecular compositional changes in live cells and detected the cellular reaction due to virus invasion three hours after infection. Virus infection was also investigated with transmission electron microscopy (TEM) to confirm viral propagation and the morphological changes in the sub-micro structure of the cells.

GENERAL INTRODUCTION: BIOLOGY OF VIRUSES

It is said that a virus is not alive because it is not able to propagate by itself. Viruses require live host cells for proliferation and use the gene duplication and protein translation systems of the host cells to replicate. Studies on viruses began at the end of the 19th century. The first virus studied was tobacco mosaic virus (TMV). Adolf Mayor is often regarded as the person who discovered TMV. He described the disease and the symptoms of TMV in a paper published in 1886, but he was not able to determine the true identity of the disease agent. The first report that unveiled the eccentric properties of this disease agent was published by Stanley in 1935. Stanley succeeded in making a crystal that had over 100-fold higher activity than the suspension of ground diseased leaves. As the manuscript described "Here we have the first demonstration that an agent which has some of the properties we associate with living organisms can be crystallized like a chemical." The result was astonishing in that the virus was neither alive nor a thing.[1]

One of the reasons for my fascination with viruses, and the impetus for this project, is that they cause many important infectious diseases. Viruses have been attributed as the cause of many diseases so far, including lethal diseases like Ebola hemorrhagic fever and intractable diseases like acquired immune deficiency syndrome (AIDS), as well as epidemics such as hepatitis, yellow fever, poliomyelitis and smallpox. Some viruses are known as oncoviruses, which promote certain forms of cancer.[2] Cervical cancer is attributed to human papilloma virus.[3] A study suggested that approximately 15% of all tumors in humans are a consequence of a virus infection.[4] Therefore, a technique for virus detection is necessary to reduce the number of victims. One of the important and interesting properties of viruses is the high specificity to the species infected. Since viral host specificity is high, it is a rare occurrence that a human infectious virus infects other

animals, for example, monkeys.[5] The host-specific properties of the virus are attributed to the mechanism of virus adsorption onto the host cell. When viruses make contact with the cell, they bind to receptors on the cell surface. For example, the main receptor of the human immunodeficiency virus (HIV)-1 and HIV-2 is the CD4 protein on T cells. In the case of HIV, viruses also use co-receptors to invade the cellular membrane. The high specificity of the virus is attributed to the affinity of the ligand-receptor interaction,[6] which makes it very difficult to study viral diseases. There is another problem in viral research, pathogenic strength. Feline immunodeficiency virus (FIV) is a lentivirus inducing AIDS-like symptoms in cats.[7] There is FIV for puma-derived species of cat FIV, but it is non-pathogenic for pumas.[8] Consequently, it is not possible or efficient to use animals to detect and study human infectious viruses.

The above difficulty induced me to come up with the idea of using a human culture cell as a detector of human infectious viruses. Currently, there is no means to detect a human infectious virus without getting infected. A doctor assumes the type of virus according to the symptoms of the patient, such as cough, sneeze, fever, pain, etc. The doctor uses a kit designed for a specific virus to confirm its existence. As the kit usually utilizes an immunostaining technique, one kit is applicable to one type of the virus and is not able to identify the other types of viruses. If a virus infection in a cell in a cultural dish could be detected, no patient would be necessary and any human infectious virus could be detected. The problem was how to detect it, because the cell does not have fever, cough, or any remarkable reaction. A single cell does not have an immune system. There is no morphological change that is visually recognized on the cells infected with virus in the first 24-48 h. Consequently, I came up with the idea of using Raman spectroscopy.

Conventional virology techniques rely on specific antibodies. When these methods were not successful, laboratory diagnosis remained a problem because the possible direct detection methods such as analysis of nucleic acids or morphological observation by electron microscopy have low capability to detect a virus. The requirements including the time required to detect the specific immune response and the interpretation of antibody values for viruses that cause latent infections, have caused continuing diagnostic dilemmas for the clinical virologist. The conventional methods for the detection of virus including electron microscopy, antigen detection, and virus isolation in cell culture, have recently been reviewed.[9-10] Electron microscopy is utilized for the detection of virus in cellular samples but is not sensitive and requires time consuming sample preparation.[11-12] The method often used is one based on direct antigen identification including immunofluorescence, radioimmunoassay, and ELISA techniques.[13-15] These techniques are commonly used for direct antigen identification to detect the viral infection in human patients.[16] Since these methods detect antibodies made by the patient's immune system, they are not applicable in the present patient-less viral detection technique; besides, they do not detect the virus directly. The gold standard for identification of virus types is the method using several types of cultured human and some animal cells. The viral type is suggested with the infectious cell types. It usually takes 1-2 weeks to confirm virus propagation in the cells, which is detected by morphological changes of the cells, referred as a cytopathic effect (CPE). Additional methods using polymerase chain reaction (PCR) or immune reactions are often applied for the identification of several types of viruses. Although these methods provide direct evidence of the virus, they require trained operators and are costly. Also, these methods have high specificity to the virus type. However, these tests are less sensitive without using the cell culturing technique that is still the most

commonly used method in virology. The above methods are time-consuming for sample preparation and are not sufficient for real-time analysis.

The commonly used diagnosis methods for HIV and HCV infection are achieved by the detection of antibodies in human patients. These viruses are able to transmit vertically from mother to child but it is difficult to diagnose the infection in the baby. The passive acquisition of maternal antibody confuses confirmation of infection in the neonate. The serological diagnosis of HIV and HCV infection is also difficult during the "window period" in which the virus infection has not yet been recognized by the immune system and antigen is not yet produced. This poses a concern for the safety of blood products: an estimated risk of HCV transmission.[17] Consequently, a technique to detect human infectious virus without human patients is strongly required.

Raman spectroscopy is one of the powerful and promising tools to analyze live cells at the molecular level. Raman spectroscopy is widely used for the determination and detection of molecules in a totally noninvasive and label-free manner. Raman scattering occurs when light interacts with molecular vibrations and changes in the polarizability take place in the molecular vibrational motion. It results in light scattering with an energy shift (up or down) that is equal to the molecular vibrational energy and is regarded as an inelastic collision between the photon and the molecule. The spectroscopic profile of Raman scattering arises from all Raman-active vibrational modes at once in molecules such as nucleic acids, proteins, lipids, carbohydrates, etc.. Therefore, it is not necessary to label any molecule to observe it. In contrast, a sample consisting of many materials, such as cells and tissue, shows a complicated Raman spectrum that includes all Raman bands overlapping each other.

Sir C. V. Raman published a paper “A new radiation” in 1928; he was awarded the Nobel Prize in physics in 1930. He used filtered sunlight to excite solvents and photographic plates were used to record the spectrum. It took about 24 h to record the spectrum of a beaker with ca. 600 mL of pure liquid.[18] Puppels et al. introduced a Raman microscope that had combined Raman spectroscopy with an optical microscope in 1990.[19] It provides a huge contribution to research on single cells and tissues *in vitro*. The technical progress in lasers, charge-coupled device detectors, and fiber-optic probes brought Raman spectroscopy to the field of biomedical science. The large progression in biomedical Raman spectroscopy was possible by the use of multivariate analysis techniques.[20] These techniques allow one to extract valuable information from the complex Raman spectra of the biological samples.

Infrared (IR), near infrared (NIR) and Raman spectroscopies are categorized as vibrational spectroscopy. They are also powerful tools to study biological samples. However IR and NIR have a weak point in live cell analysis from interference due to water. The strong absorption bands of water conceal the bands of the samples over a wide spectral range, including the fingerprint region. These techniques are often used for the observation of dried and stained biological samples. Although water has a strong band in the Raman spectrum also, the band due to water appears at a high frequency region from 3000 to 3800 cm-1, in which very few chemical substituent groups, such as NH, have their vibrational modes. Also, since Raman spectroscopy uses light in the visible-NIR range, 400-1000 nm, it is easy to combine with an optical microscope. Raman spectroscopy provides enough high spatial resolution and resistance to water content in live cells and tissues; thus, it is a powerful tool for noninvasive and real-time analysis of biological samples.[21] The major drawback in the Raman technique is the low cross-section of the Raman scattering effect.

Raman spectroscopy has been applied for analyses of bacteria, viruses, mammalian cells, and cellular organelles.[22-24] The spatial resolution of the Raman microscope has significantly improved with the combination of the Raman microscope and the confocal setup, in that the confocal Raman microscope allows the collection volume of less than 1×1×5 μm to study phenomena occurring in the limited small size of the live single cell.[25-29]

REFERENCES

1. Zaitlin M., The Discovery of the Causal Agent of the Tobacco Mosaic Disease: Chapter 7. Discoveries in Plant Biology 105-110 (1998).
2. Parkin, D.M., The global Health Burden of Infection-associated Cancers in the year 2002. Int J Cancer 118: 3030-44 (2006).
3. Beibei, L., Viscidi, R.P., Lee, J.H., et al. Human Papillomavirus (HPV) 6, 11, 16, and 18 Seroprevalence Is Associated with Sexual Practice and Age: Results from the Multinational HPV Infection in Men Study (HIM Study). Cancer Epidemiol Biomarkers Prev 20: 990-1002 (2011).
4. Anand, P., Kunnumakkara, A.B., Kunnumakara, A.B., Sundaran, C., Harikumar, K.B., Tharakan, S.T., Lai, O.S., Sung, B., Aggarwal, B.B., Cancer is preventable disease that requires major lifestyle changes, Pham. Res. 25:2097-116 (2008).
5. JM Conly, and BL Johnston, The infectious diseases consequences of monkey business Can J Infect Dis Med Microbiol. 19(1): 12–14 (2008).
6. Andrew W. Woodham, PhD, Joseph G. Skeate, MS, Adriana M. Sanna, MSc, Julia R. Taylor, BS, Diane M. Da Silva, PhD, MS, Paula M. Cannon, and W. Martin Kast, Human Immunodeficiency Virus Immune Cell Receptors, Coreceptors, and Cofactors: Implications for Prevention and Treatment AIDS Patient Care STDS. 2016 Jul 1; 30(7): 291–306.
7. John H. Elder, 1 Ying-Chuan Lin,1 Elizabeth Fink,Feline Immunodeficiency Virus (FIV) as A Model for Study of Lentivirus Infections: Parallels with HIV Curr HIV Res. 2010 Jan; 8(1): 73–80.
8. Jennifer J. H. Reynolds, Scott Carver, Mark W. Cunningham, Ken A. Logan, Winston Vickers, Kevin R. Crooks, Sue VandeWoude, and Meggan E.

Craft Feline immunodeficiency virus in puma: Estimation of force of infection reveals insights into transmission Ecol Evol. 9(19): 11010–11024 (2019).

9. Diane S. LelandMorris, French L. V., Diagnosis of Infectious Diseases Principles and Practice,Virus Isolation and Identification Laboratory 39-59 (1988).
10. Fenner's Veterinary Virology (Fourth Edition), Chapter 5 - Laboratory Diagnosis of Viral Infections 101-123(2011)
11. Zhang Ying , Hung Tao, Song Jing Dong and HE JinSheng Electron microscopy: essentials for viral structure, morphogenesis and rapid diagnosis Science China, Life Sciences May 2013 Vol.56 No.5: 421–430
12. D. S. Leland and C.C. Ginocchio. Clinical Microbiology "Role of Cell Culture for Virus Detection in the Age of Technology," 20, 49-78 (2007)
13. M.D. Omrani, M. H. K. Ansari and D. Agaverdizadae "PCR and Elisa Methods (IgG and IgM): Their Comparison with Conventional Techniques for Diagnosis of Mycobacterium Tuberculosis" Pakistan Journal of Biological Sciences, 12 (4): 373-377, (2009)
14. J. E. Cradock-Watson, M. K. Ridehalgh, J. R. Pattison, M. J. Anderson, and H. O. Kangro "Comparison of immunofluorescence and radioimmunoassay for detecting IgM antibody in infants with the congenital rubella syndrome", J Hyg (Lond), 83(3) 413–423, 1979
15. L Rodak, L A Babiuk, and S D Acres Detection by radioimmunoassay and enzyme-linked immunosorbent assay of coronavirus antibodies in bovine serum and lacteal secretions. J Clin Microbiol. 1982 Jul; 16(1): 34–40.
16. W. S. M. William, A. E. Tollefson, "Adenovirus methods and protocols. Ad proteins, RNA, lifecycle, host interactionnetics, and phylogenetics," Second

Edition, 2, Chap. 21 in Characterization of the Adenovirus Fiber Protein, pp. 288-289, Humana press, Totowa, New Jersey (2007).

17. Sherman, K.E., Shire, N.J., Cernohous, P., Rouster S.D., Omachi J.H., Brun, S., Da Silva, B. Liver injury and changes in hepatitis C Virus (HCV) RNA load associated with protease inhibitor-based antiretroviral therapy for treatment-naive HCV-HIV-coinfected patients: lopinavir-ritonavir versus nelfinavir. Clin Infect Dis. 41(8):1186-95 (2005). (2005)
18. Peter Vandenabeele "Practical Raman Spectroscopy: An Introduction", 2013 John Wiley & Sons, Ltd.
19. Pupples G. J., F.F. de Mul, C. Otto, J. Greve, M. Robert – Nicoud, D. J. Arndt – Jovin, and T. M. Jovin. "Studying single living cells and chromosomes by confocal Raman microscopy," J. Nature 347, 301-303 (1990).
20. Pu Chen, Aiguo Shen, Xiaodang Zhou and Jiming Hu. "Bio-Raman spectroscopy: a potential clinical analytical method assisting in disease diagnosis", J.Anal. Meth., 3, 1257-1269, 2011
21. Jeremy D. Driskell, Yu Zhu, Carl D. Kirkwood, Yiping Zhao, Richard A. Dluhy, Ralph A. Tripp, "Rapid and sensitive detection of rotavirus molecular signatures using surface enhanced Raman spectroscopy", 5(4), e10222, (2010)
22. Jeremy D. Driskell, Yu Zhu, Carl D. Kirkwood, Yiping Zhao, Richard A. Dluhy, Ralph A. Tripp, "Rapid and sensitive detection of rotavirus molecular signatures using surface enhanced Raman spectroscopy", Plos one/www.plosone.org, April 2010, 5(4), e10222
23. K. Hamasha, Q. I. Mohaidat, R. A. Putnam, R. C. Woodman, S. Palchaudhuri, S.J. Rehse, "Sensitive and specific discrimination of pathogenic and nonpathogenic

Escherichia coli using Raman spectroscopy—a comparison of two multivariate analysis techniques," Biomed Opt Express., **4**(4) 481–489 (2013).

24. J. D. Driskell, Y. Zhu, C. D. Kirkwood, Y. Zhao, R. A. Dluhy, R. A. Tripp, "Rapid and sensitive detection of Rotavirus molecular signatures using surface enhanced Raman spectroscopy," J. PlOS ONE, 5(4), 1-9 (2010).
25. L. Kong, P. Zhang, P. Setlow, Yong-qing Li, "Multifocus confocal Raman microspectroscopy for rapid single-particle analysis," J. Biomed Opt., 16(12), 120503-12506 (2011).
26. K. Hamada, K. Fujita, N. I. Smith, M. Kobayashi, Y. Inouye, S. Kawata, "Raman microscopy for dynamic molecular imaging of living cells," J. Biomed. Opt. 13(4), 044027-044031 (2008).
27. C. Matthaus, A. Kale, T. Chernenki, V. Torchilin, M. Diem, "New ways of imaging uptake and intracellular fate of liposomal drug carrier system inside individual cells, based on Raman microspectroscopy," J. Mol. Pharmaceut., **5**(2), 287-293 (2007).
28. S. S. Biel, A. Nitche, A. Kurth, W. Siegert, M. Ozel, H. R. Gelderblom, "Detection of human polyomaviruses in urine from bone marrow transplant patients: comparison of electron microscopy with PCR," J. Clin. Chem. **50**, 306-312(2004).
29. Francisco J. Ramirez, Belen Nieto-Ortego, Juan Casado and Juan T. Lopez Navarrete, "The first chiral Raman spectrum report of a protein: a perspective of 20 years" J. Chem. Commun., 2013(49), 8893-8895.

Chapter 1

Noninvasive and label-free determination of virus infected cells by Raman spectroscopy

ABSTRACT

The present study demonstrates that Raman spectroscopy is a powerful tool for the detection of virus-infected cells. Adenovirus infection of HEK293 cells was successfully detected at 12, 24, and 48 h after initiating the infection. The score plot of principal component analysis (PCA) discriminated the spectra of the infected cells from those of the control cells. The viral infection was confirmed by the conventional immunostaining method performed 24 h after the infection. The newly developed method provides a fast and label-free means for the detection of virus-infected cells.

INTRODUCTION

Raman spectroscopy is a promising technique for the analysis of biomedical samples. The use of the Raman microscope enabled direct measurements of single live cells. During the past few decades, Raman spectroscopy has been used for bacterial identification. Using Raman spectroscopy, Kastanos *et al.* [1] identified various strains of bacteria found in urinary tract infections: 25 strains of *E. coli*, 25 strains of *K. pneumonia*, and 25 strains of *Proteus spp*. Raman spectroscopy is also used for identification of mycobacterium.[2] Previous studies have demonstrated that Raman spectroscopy provides sufficient information to identify specific microorganisms.[3-5] Raman spectroscopy has also been applied to the analysis of cells. Notingher *et al.* used a Raman microspectrometer to characterize living cells attached to bioinert silica materials[6]. Oshima *et al*. measured Raman spectra of single live human lung cancer cells and successfully discriminated them by multivariate analysis.[7] Earlier studies revealed that even minor alterations that occur in living cells could be detected using Raman spectroscopy in a totally noninvasive and label-free manner. Further, Raman spectroscopy has also been used to study the structures of proteins, nucleic acids, and other components of virus, including conformational changes during viral procapsid and capsid assembly.[8, 9] Viral infections lead to many diseases, including certain forms of cancers.[10-12] Recombinant viruses can be fluorescently labeled, e.g., with GFP, to allow for the detection of infected cells in in vitro studies. Alternatively, immunostaining can also be used for their detection. [13, 14] However, these conventional methods are effective only if the type of virus under investigation is known in advance. Therefore, we cannot detect an unknown virus even if it has human infectability. We can confirm the existence of the human infecting virus only when a person has been infected

by it. Therefore, development of new techniques for the identification of pathogenic viruses is highly desirable.

The purpose of the present study was to examine the viability of Raman spectroscopy for the label-free detection and discrimination of virus-infected cells. To this end, I employed a recombinant adenovirus that lacks the E1 gene and HEK293 cells harboring this factor. Since the E1 factor was necessary for reproduction of the virus, this virus cannot proliferate in normal human cells that lack this factor, making the present study safe.

EXPERIMENTAL

a. Preparation and culture of virus-infected cells

Human embryonic kidney epithelial (HEK293) cells were purchased from DS Pharma Biomedical (Japan). The HEK293 cells were cultured in high-glucose Dulbecco's Modified Eagle Medium (DMEM; WAKO, Japan) supplemented with 10% fetal bovine serum (FBS; Beit HAEMEK, LTD., Israel) and 100 IU/mL penicillin (WAKO, Japan). The cells were maintained at 37°C and 5% CO_2 in a humidified incubator. A special dish with a quartz window at the bottom purchased from Synapse-Gibko (Japan) was used for

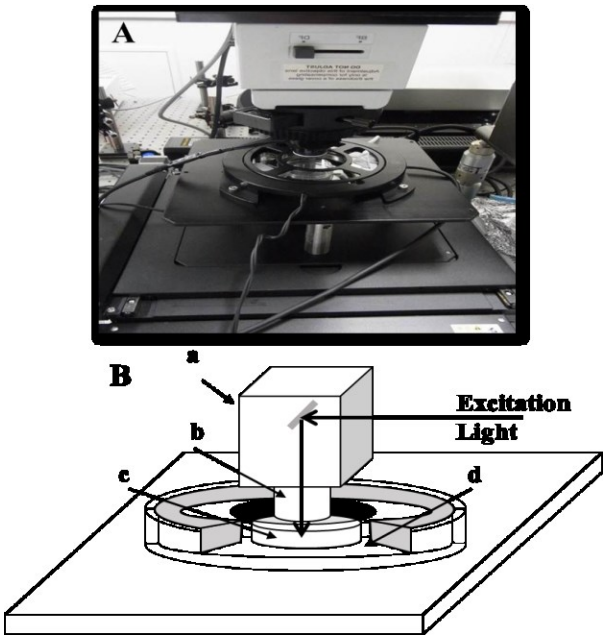

Fig. 1 Photograph (A) and scheme (B) of the sampling stage of Raman microscope. The stage consists of microscope (a), objective lens (b), culturing dish (c), and indium tin oxide glass heater (d).

Raman measurements. Adenovirus (Ad-CMV-control) stock was prepared according to reported methods.[15] The virus was stored at −80°C until use. The viral titer used was 0.5 × 10^6 PFU/mL, and the multiplicity of infection (MOI) was 6 PFU/cell. The viral infection was confirmed by immunostaining. A rabbit polyclonal antibody (anti-72K Ab) was employed, which detected the E2 polypeptide of the adenovirus. For fluorescence imaging, fluorescein isothiocyanate (FITC)-labeled antibody, which detected rabbit IgGs, was used. The fluorescent images were captured using a Nikon A-1 (Nikon, Japan) confocal fluorescence microscope.

b. Raman measurements

Raman measurements were made using a confocal Raman microscope (Nanofinder, Tokyo Instruments, Japan). The system had a CO_2 incubator, which maintained the culture dishes at 37°C in an atmosphere of 5% CO_2 during the measurements (Fig. 1). A continuous wave background-free electronically tuned Ti:sapphire laser (CW-BF-ETL; Mega Opto, Japan) provided an excitation beam of 785 nm wavelength. The laser power was typically set to 30 mW during sampling. The exposure time was 30 s × 3 times. The microscope was equipped with a ×60 water-immersion objective lens (NA = 1, 10, Olympus, Japan), a Raman polychromator equipped with a grating (600 l/mm, 750 nm-blazed), and a Peltier-cooled CCD detector (DU-401-BR-DD, Andor Technology, Ireland). The spectral resolution was 5 cm^{-1}. The measurements were made 12, 24, and 48 h after the addition of the virus. To measure the spectra, the laser was focused into the nucleus of the cells. The spectra were collected from approximately 12 randomly selected cells in each dish. The spectrum of the cell was processed by background subtraction and 6^{th} polynomial fitting to remove the artifacts from the culturing media and the dish window.

The Raman spectra of cells were processed by principal component analysis (PCA). The intensities of the spectra were normalized using a band at 1003 cm^{-1} of phenylalanine or a band at 1440 cm^{-1} assigned to a CH deformation mode. Multivariate analysis software, Unscrambler (CAMO, Norway), was used for further analysis. The data was mean centered before the PCA.

RESULTS AND DISCUSSION

Microscopic images of HEK293 cells without (a) and with (b) virus after 48 h of cultivation are shown in Fig. 2A and 2B. The density of the cells appears different in the images but it is unrelated to the virus. Quinlan and Grodzicker reported that the adenovirus starts proliferating in the cells within 12 h.[16] However, viral infection could not be assessed by observing the morphological changes of the cells, and no apparent changes in morphology were observed during infection. Apoptotic or necrotic cells were not found when examined 48 h after the addition of the virus.

Figure 2C shows a fluorescence image of the cells 24 h after the addition of virus. The intensity of fluorescence was proportional to the amount of E2 polypeptide in the cells. The images indicated that the virus proliferated in 5%–10% of the cells that showed intense fluorescence emission. Weak fluorescence observed in other cells was probably

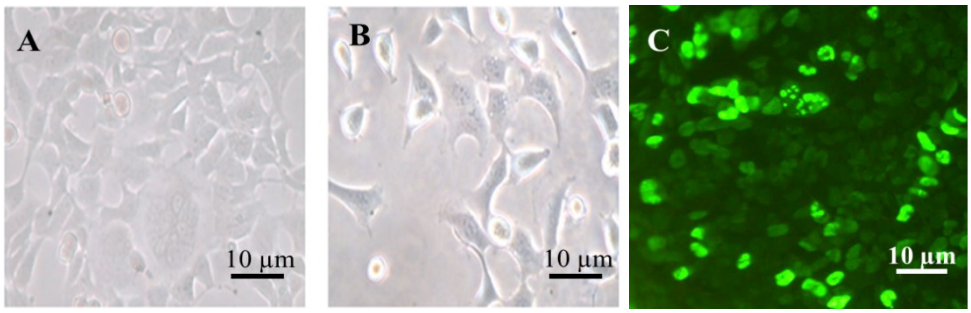

Fig. 2 Bright field images of HEK293 cells without (a; control) and with virus (b) 48 h after the virus addition. Fluorescence images of immunostained HEK293 cells with virus observed 24 h after virus addition (c).

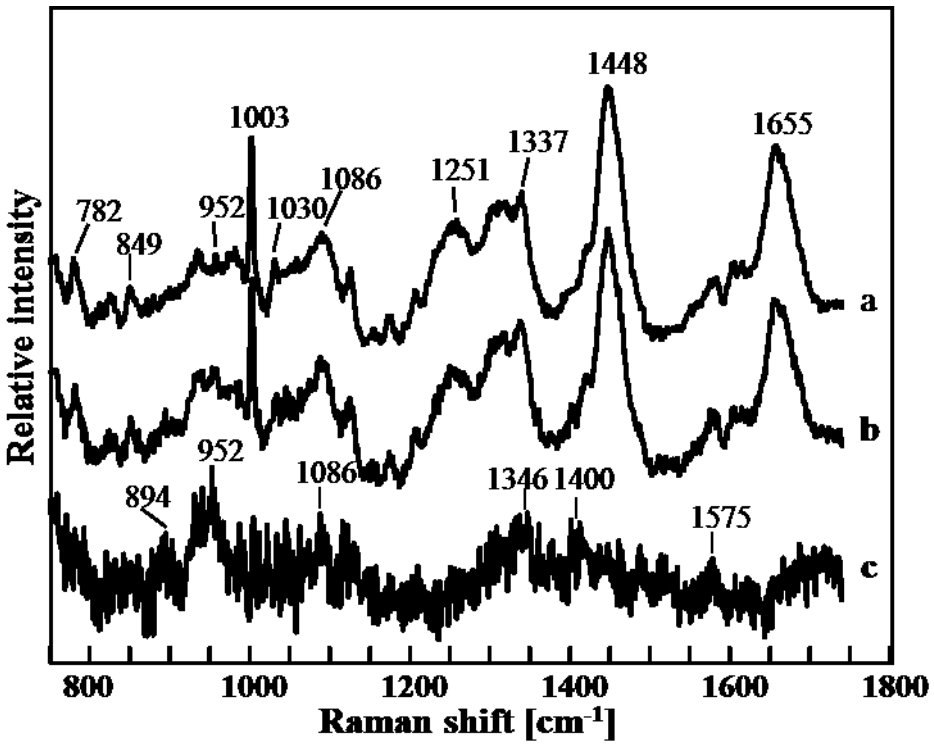

Fig. 3 Averaged Raman spectra of cells without (a) and with (b) virus, and their difference spectrum [(c); (a) and (b)]. Raman spectra of HEK293 without (a) and with (b) virus, and their difference spectrum (c) are shown in

due to low concentration of the E2 polypeptide produced, suggesting that the virus had not proliferated in these cells. Raman spectra of HEK293 without (a) and with (b) virus, and their difference spectrum (c) are shown in Fig. 3. The spectra were measured 48 h after the virus addition. The spectra measured 12 and 24 h after the virus addition are not shown, because characteristic differences were minimal. Bands at 1651, 1450, and 1335 cm^{-1} were assigned to amide I, CH bending, and amide III modes of proteins. A sharp band at 1003 cm^{-1} and a minor band at 1030 cm^{-1} were attributed to phenylalanine in the proteins. Bands at 1090 cm^{-1} were assigned to a symmetric stretching vibration mode of phosphate and that at 853 cm^{-1} was assigned to DNA. These bands were clearly observed in the difference spectra, suggesting that the adenovirus infection significantly altered the concentration or composition of nuclear DNA. The Raman spectra of control cells (without virus) were

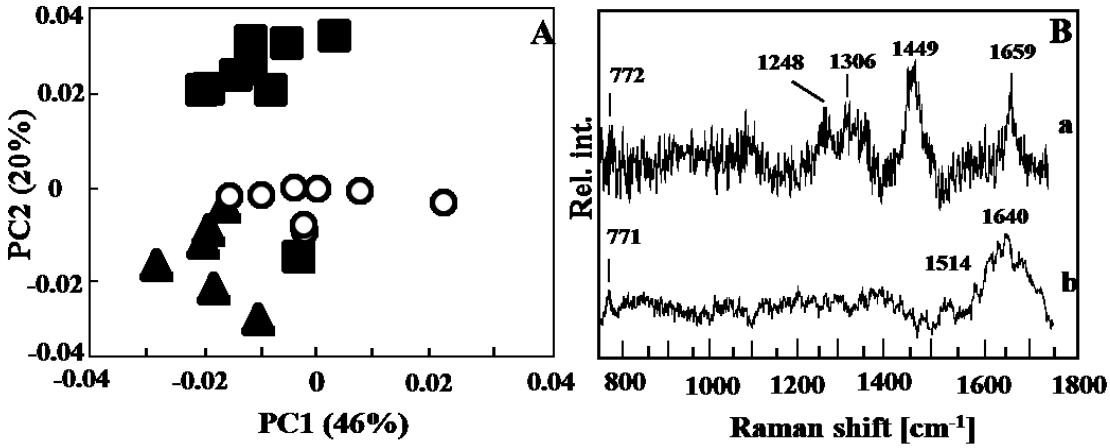

Fig. 4. Score plot (A) and loading plots (B) of principal component analysis (PCA) model constructed for the three control datasets collected 12 h after virus addition. The datasets obtained from the first (open circle), second (filled triangle), and third (filled square) experiments are plotted in the score plot for PC 1 and PC 2. The loading plots are depicted for PC 1 (a) and PC 2 (b).

subjected to PCA (Fig. 4). Since we repeated the same experiments three times, the three datasets were expected to make a single distribution.

As shown in the score plot (Fig. 5A), the datasets for different days formed independent groups, suggesting that the HEK293 cells were sensitive to subtle changes in the culture conditions, which could not be controlled. The loading plot (Fig. 5B) for PC1 showed a strong contribution of free water near 1640 cm^{-1}(Fig. 4B). Therefore, the spectral region from 1550 to 750 cm^{-1} was selected for subsequent analysis to suppress the interference arising from changes in experimental conditions. A score plot of PCA of the spectra of cells with and without virus 12 h after the addition of virus is shown in Fig. 5A. Up to seven PCs were obtained and the PCA score plot was composed of two characteristic PCs, with major differences between these two groups. The data sets of cells with and without virus showed significant differences. At the border area, some of the data from the virus-treated group overlapped with that of cells not treated with virus. The control (cell-without-virus) data separated into two groups along the PC 2 axis, which can be attributed

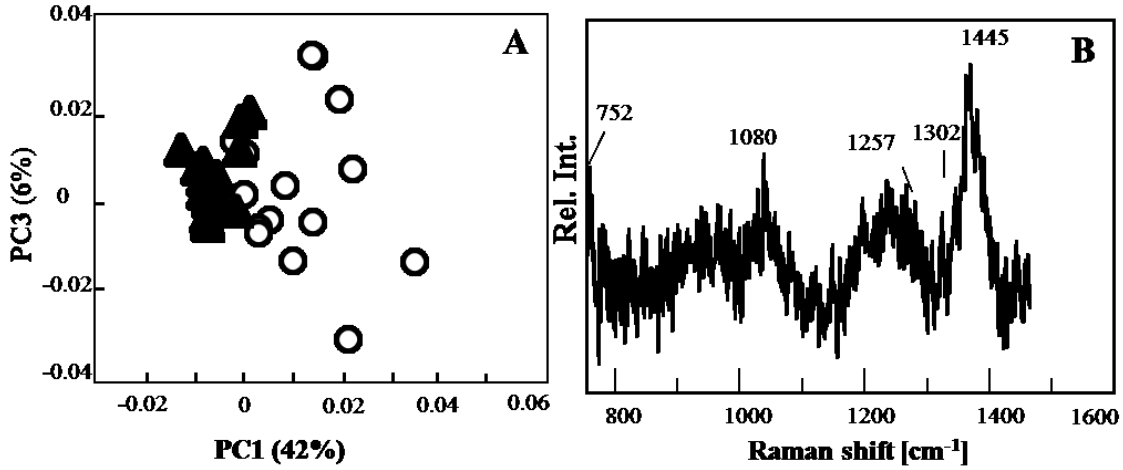

Fig. 5 Score plot (a) and loading plot (b) of PCA model constructed for the dataset collected 12 h after virus addition. The data from the control (open circle) and from a cell with the virus (filled triangle) are plotted in the score plot composed of PC 1 and PC 3. The loading plot is depicted for PC 1.

to the fluctuating culture conditions. As described earlier, this data was collected from three independent experiments. When PCA was carried out for each experimental dataset, these three datasets highlighted consistent differences with high reproducibility. Loading plots for PC 1 (a) and PC 2 (b) are shown in Fig. 5B. Bands at 1445 and 1302 cm^{-1} in PC 1 were observed in the positive direction, which may be attributed to changes in the composition of lipids. Bands at 1257, 1080, and 752 cm^{-1} were attributed to DNA. The PCA score plot for the spectra recorded 24 h after the virus addition is shown in Fig. 6A. PC 1 (not shown) was unrelated to viral infection, and was probably due to variations in culture conditions. PC 2 contributed to the discrimination of two groups. Very few spectra of the cell-with-virus group were classified into the cell-without-virus group, suggesting that the virus infection progressed and most of the cells had already sensed the virus invasion. The control (cell-without-virus) data separated into two groups along the PC 3 axis, which was attributed to the fluctuation of culturing conditions. The loading plot of PC 2 is shown in Fig. 6B. The noisy nature of the plot suggested that the differences between

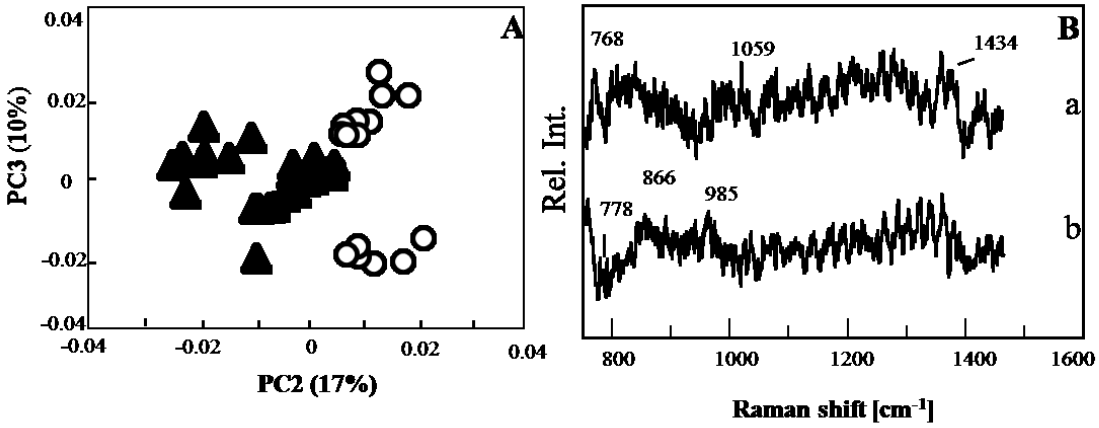

Fig. 6 Score plot (A) and loading plot (B) of PCA model constructed for the dataset collected 24 h after virus addition. The data from the control (open circle) and from a cell with the virus (filled triangle) are plotted in the score plot composed of PC 2 and PC 3. The loading plots are depicted for PC 2 (a) and PC 3 (b).

spectra without and with virus were considerably small. A weak and broad band near 1440 cm^{-1}, which was almost buried in noise, was probably due to a CH bending mode. Bands at 985 and 866 cm^{-1}, observed in the positive direction, were due to polysaccharides. A positive band near 750 cm^{-1} was attributed to DNA. The PCA score plot for spectra 48 h after the virus addition is shown in Fig. 7A. The plot showed good discrimination between two groups within the PC 2 axis. There was some overlap between the two groups. The loading plot of PC 2 is shown in Fig. 7B(b). A negative band near 1440 cm^{-1} was due to the CH bending mode. A positive band at 952 cm^{-1} was assigned to the PO_4^{3-} group. This band suggested that the normal uninfected cells had more Ca^{2+} ions than did the virus-infected cells. The features of the loading plots for the cells 12, 24, and 48 h after the virus addition were different, which appeared to reflect the dynamics of the reaction of the cells. During the early stages of infection (less than 12 h), several cells with virus were found to be classified into the group of cells without virus, because the virus had not yet succeeded in invading these cells. At 24 h, the overlap between the groups of cells with and without the virus was much smaller. It appears that the spectral changes reflected the self-defense

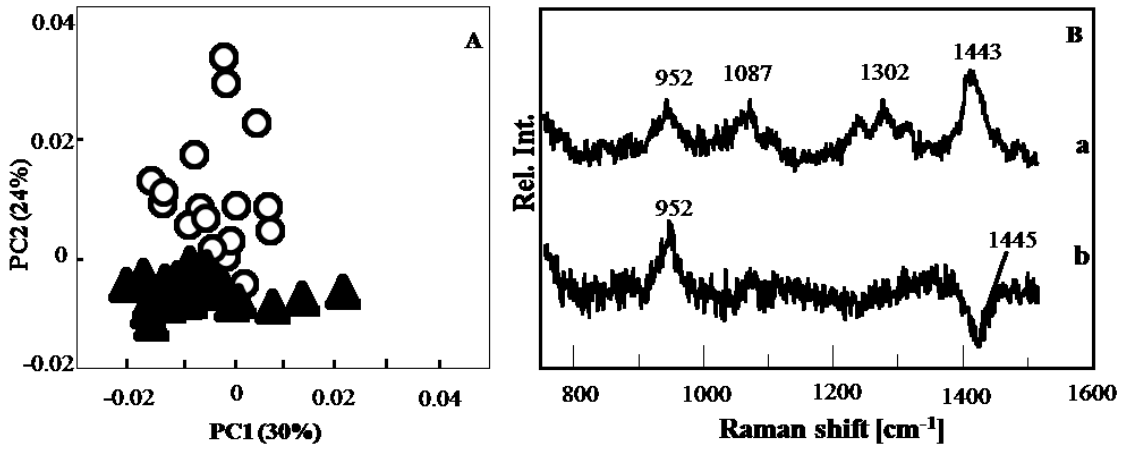

Fig. 7 Score plot (A) and loading plot (B) of PCA model constructed for the dataset collected 48 h after virus addition. The data for the control (open circle) and from a cell with the virus (filled triangle) are plotted in the score plot composed of PC 1 and PC 2. The loading plots are depicted for PC 1 (a) and PC 2 (b).

reaction of the cells to the virus infection. As evident from the fluorescence images, in the cells, the virus started replicating 48 h after its addition. The noise level in PC 2 of the data collected 48 h after virus addition was much lower than those corresponding to data collected after 12 and 24 h, indicating a much larger spectral alteration. The PCA analysis showed that the concentration of the PO_4^{3-} group was lower in the virus-infected cells. Therefore, the bands corresponding to the PO_4^{3-} group may be used as a marker of virus proliferation inside the cells. The analysis of fluorescence emission showed that 5%–10% of the cells emitted intense fluorescence, whereas the Raman analysis classified nearly 100% of the cells into the infected group. Judging from the MOI (6 PFU/cell), 6 virus particles were used to infect one cell, a ratio sufficiently high to ensure that all cells are infected. Therefore, the Raman analysis was more sensitive in detecting the viral infection than the conventional fluorescence imaging methods.

CONCLUSION

The present study demonstrates that Raman spectroscopy can be used for sensitively detecting viral infections in live cells without any labeling. The viral infection was detected 12 h after incubating the cells with the virus. Further, Raman spectroscopy is a faster method for the detection of viral infection than the conventional immunostaining method. The newly developed method does not require specific information on the virus for the analysis. The spectral changes observed 12 and 24 h after virus addition are probably due to the defense response of the cells to infection. The spectral changes observed 48 h after the addition of the virus were probably due to a combination of virus proliferation and defense response. The band at 952 cm^{-1} attributed to the PO_4^{3-} group was found to be a good marker for the proliferation of the virus in the cells.

REFERENCES

1. E. Kastanos, A. Kyriakides, K. Hadjigeorgiou, and C. Pitris, "A Novel Method for Bacterial UTI Diagnosis Using Raman Spectroscopy," *International Journal of Spectroscopy* 2012, 1-13 (2012).
2. P.C. Buijtels, H.F. Willemse-Erix, P.L. Petit, H.P. Endtz, G.J. Puppels, H.A. Verbrugh, van A. Belkum, van D. Soolingen, K. Maquelin, "Rapid identification of mycobacteria by Raman spectroscopy," *J. Clin Microbiol.* 46(3), 961-965 (2008).
3. F. Jamal, M. Almarashi, N. Kapel, T. S. Wilkinson, and H. H. Telle, "Raman Spectroscopy of Bacterial Species and Strains Cultivated under Reproducible Conditions," *Spectroscopy: An International Journal* 27(5-6), 361-365 (2012).
4. L. P. Maquelin, H. P. Choo-Smith, H.A. Endtz, A. Bruining, and G. J. Puppels, "Rapid identification of Candida species by Confocal Raman microspectroscopy," *Journal of Clinical Microbiology* 40(2), 594-600 (2002).
5. S. Meisel, S. Stöckel, M. Elschner, F. Melzer, P. Rösch, and J. Popp,"Raman Spectroscopy as a Potential Tool for Detection of *Brucella* spp. in Milk.," *Appl Environ Microbiol.* 78(16), 5575–5583 (2012).
6. Notingher, J. R. Jones, S. Verrier, I. Bisson, P. Embanga, P. Edwards, J. M. Polak, and L. L. Hench, "Application of FTIR and Raman spectroscopy to characterisation of bioactive materials and living cells," *Spectroscopy* 17(2-3), 275-288 (2003).
7. Y. Oshima, H. Shinzawa, T. Takenaka, H. Sato, C. Furihata, "Discrimination analysis of human lung cancer cells associated with histological type and malignancy using Raman spectroscopy," *J. Biomed. Opt*. 15(1), 017009 (2010).

8. J.M. Benevides, J.T. Juuti, R. Tuma, D. H. Bamford, and G.J. Thomas, "Characterization of subunit-specific interactions in a double-stranded RNA virus: Raman difference spectroscopy of the phi6 procapsid," *Biochemistry* 41(40), 11946-11953 (2002).
9. R. Tuma, G.J. Thomas, "Mechanisms of virus assembly probed by Raman spectroscopy: the icosahedral bacteriophage P22, "*Biophys. Chem.* 68(1-3), 17-31 (1997).
10. Schafer, D. Lengenfelder, C. Grillhosl, C. Wieser, B. Fleckenstein, A. Ensser,"The latency-associated nuclear antigen homolog of herpesvirus saimiri inhibits lytic virus replication," *J. Virol.* 77, 5911–5925 (2003).
11. E. Vargis, Y.W. Tang, D. Khabele, and A. M. Jansen," Near-infrared Raman Microspectroscopy Detects High-risk Human Papillomaviruses," *Transl. Oncol.* 5(3) 172–179 (2012).
12. M. Relhan, M. Heikenwalder, U. Protzer,"Direct Effects of Hepatitis B Virus-Encoded Proteins and Chronic Infection in Liver Cancer Development," *Dig Dis.* 31(1) 138-151 (2013).
13. W. S. M. William, A. E. Tollefson, "Adenovirus Methods and Protocols. Ad Proteins, RNA, Lifecycle, Host Interactionnetics, and Phylogenetics," Second Edition, 2, *Chap. 21 in Characterization of the Adenovirus Fiber Protein,* pp. 288 – 289, Humana press, Totowa, New Jersey (2007).
14. J. A. Kramps, J. Magdalena, J. Quak, K. Weerdmeester, M. J. Kaashoek, M. A. Maris-Veldhuis, F. A. Rijsewijk, G. Keil, and J. T. van Oirschot, "A simple, specific, and highly sensitive blocking enzyme – linked immunosorbaent assay for

detection of antibodies to bovine herpesvirus 1," *J. Clin. Microbiol.* 32(9) 2175–2181 (1994).

16. K. Ohtani, A. Tsujimoto, M. Ikeda and M. Nakamura, "Regulation of cell growth-dependent expression of mammalian CDC6 gene by the cell cycle transcription factor E2F," *J. Oncogene* 17(14) 1777-1785 (1998).
17. M. P. Quinlan and T. Grodzicker, "Adenovirus E1A12S protein induces DNA synthesis and proliferation in primary epithelial cells in both the presence and absence," *J. Virol.* 61(3) 673 -682 (1987).

Chapter 2

Early Detection of Virus Infection in Live Human Cells in Using Raman Spectroscopy

ABSTRACT

Virus infection of a human cell was determined only 3 h after invagination. I used viral vector Ad-CMV-control (AdC), which lacks the *E1* gene coding for early polypeptide 1 (E1). AdC can replicate in human embryonic kidney 293 (HEK293) cells into which the *E1* gene has been transfected. According to partial least-square regression discriminant analysis (PLSR-DA), it was assumed that two kinds of reaction take place in the cell during viral invasion. The first response of the cell was determined 3 h after the virus invasion, and the second one was determined ~9 h later. The first one seems to be due to compositional changes in DNA. Analysis of large-scale datasets strongly indicated that the second reaction can be attributed to a reduction in protein concentration or uptake of phenylalanine into the nucleus.

INTRODUCTION

Raman spectroscopy has advantages for biomedical applications because it can be used to noninvasively examine a single live cell without labeling. In my previous study, virus infection was successfully detected in individual live human cells by Raman spectroscopy within 12 h after addition of a virus into the culture medium.[1]I used a recombinant adenovirus, Ad-CMV-control (AdC), which lacks genes *E1* and *E3*, and HEK293 cells that possess the *E1* gene. And the *E2* codes for a DNA polymerase that is specific to replication of the viral genome. These genes coding early proteins are localized to the nucleus. The *E3* gene is related to suppression of the immune system. The lack of this gene has no effect on the cultured cells used in the present study. Therefore, AdC can infect and replicate in HEK293 cells. This technique has several advantages over conventional immunostaining and genetic tests for detection of human infectious viruses. It does not require any genetic or proteomic information about the virus in advance. Because it detects spectral changes in a live cell that are caused by virus infection, it is possible to monitor the virus invasion over long periods. These advantages suggest that the proposed technique is suitable for detection of human infectious viruses in many environments. Salman et al. applied Raman spectroscopy to identification of the infection of Vero cells by herpes simplex virus of type 1 (HSV1) and 2 (HSV2) and by varicella zoster virus.[2] They proposed to identify virus types at 24 h after infection. This approach shows good suitability of Raman spectroscopy for virus detection and identification, but at the same time, implies a challenging question regarding the origin of a difference in Raman spectra.

Development of a practical monitoring method for viral pathogens is important not only for prevention of a pandemic, such as pandemic of Ebola hemorrhagic fever, but also for early detection of oncogenic viral infections. By the modern diagnostic methods, it is

possible to detect the presence of a human infectious virus only when the symptoms appear in the infected people, e.g., a cough and fever. These symptoms may manifest themselves too late for prevention of fatal effects of the infection. The mainstream methods for diagnosis are based on the detection of viral antigens and/or nucleic acids of viruses, but they generally require specialized equipment and trained personnel. To reduce the costs and time, some emerging diagnostic assays have been developed, such as a proximity ligation assay, biosensor-based methods, fluorescence resonance energy transfer–based methods, microarray assays, and in particular, nanoparticle-based techniques.[3] Nevertheless, identification of the virus type in advance is necessary for an assay even by these new methods because they are based on molecular biology. Silva et al. studied the metabolism of HEK293 and 1G3 cells (an amniocyte-derived cell line) associated with adenovirus infection.[4] They observed specific uptake and secretion rates of metabolites during the virus infection by ^{1}H nuclear magnetic resonance (NMR) spectroscopy. According to their results, HEK293 and 1G3 cells show significant differences in metabolite consumption even in response to infection by the same adenovirus. This finding indicates that the cellular response totally depends on the cell type, even though the products are synthesized by the same virus. Tip-enhanced Raman spectroscopy (TERS) and surface-enhanced Raman spectroscopy (SERS) are also applied to virus detection and identification.[5-7]

The purpose of the present study is to develop a technique for detection of virus infection within a short period by Raman spectroscopy and to investigate the origin of the spectral changes. Raman spectroscopy is a powerful tool for studying reactions in intact live cells.[8-12] The Raman analysis proposed here offers an opportunity to detect unknown human infectious viruses in the absence of human patients. It works on cultured human

cells and indicates the presence of a virus within a short period. In this study, I investigate what kind of alteration Raman analysis detects during invasion of a virus. There are two possible reactions taking place in the infected cell: one is the fast reaction attributed to the response of the cell to viral invasion, and the other is much slower and involves duplication of the virus. The first reaction includes transfer of the virus into a lysosome, proteolysis, and antigen presentation. The second one includes expression of early genes and production of capsid proteins. To study the mechanism of the viral propagation, time-lapse Raman observation was conducted for 24 hours. The spectral changes were studied in more detail in comparison with my previous research. The present study may improve the methodology of virus research. Because Raman analysis can detect virus infection in a single cell, the experiment can be conducted with fewer virus particles than the minimal accessible number of virus particles during a clinical infection. Hence, the present study is important for evaluation and estimation of the feasibility of Raman spectroscopy for virus studies.

EXPERIMENTAL

HEK293 cells were purchased from DS Pharma Biomedical (Japan). The cells were cultured in high-glucose Dulbecco's modified Eagle's medium (DMEM; Wako, Japan) supplemented with 10% of fetal bovine serum (FBS; Beit HAEMEK, Ltd., Israel) and 100 IU/mL penicillin (Wako). The cells were cultured in a CO_2 incubator, SCA/SMA-163 (Astec, US), at 37°C and 5% of CO_2. A special dish with a quartz window at the bottom was purchased from Synapse-Gibko (Japan) and used for Raman analyses. A stock of an adenovirus, AdC, was prepared by the method reported in another paper.[13] The virus was stored at −80°C until experiments. The two virus stocks were used at the viral titer of 0.5×10^6 plaque-forming units (PFU)/mL. HEK293 cells were checked for mycoplasma

infection with a PCR detection kit (e-Myco VALiD, Cosmo Bio, Japan), and the result was negative.

a. Immunostaining

The infection by AdC was confirmed by indirect immunofluorescent labeling. The cells were cultured for 0, 3, 12, 24, and 48 h and were stained after the Raman spectroscopy. After careful removal of the medium, the cells were fixed with paraformaldehyde (PFA; 4%) for 10 min. After two washes with PBS without divalent cations [PBS(-)], the fixed cells were incubated with methanol (90%) for 2 min to permeabilize the plasma membrane, then washed thrice with PBS(-). The samples were incubated with antibody to a 72K viral product (1:1000) diluted in bovine serum albumin (BSA) with sodium azide, at 36.6°C for 45 min. After incubation with the primary antibody, the samples were washed thrice with PBS(-) for 5 min each. The samples were incubated with a secondary antibody at 36.6°C for 45 min, followed by washing thrice with PBS(-). The secondary antibody, anti-rabbit IgG antibody, conjugated to Alexa Fluor 546 dye was used for the observation of the samples at 0 and 3 h and that conjugated to fluorescein isothiocyanate (FITC) dye was done for those at 12, 24, and 48 h. Fluorescent images were captured using an A1 confocal fluorescence microscope (Nikon, Tokyo, Japan).

b. Raman spectroscopy

Two Raman microscopes were used in this study. They were both equipped with a CO_2 incubator that maintained the culture dishes at 37°C in an atmosphere containing 5% of CO_2 during the measurements. One of them, Nanofinder (Tokyo Instruments, Japan) is

equipped with an upright microscope. Its water immersion objective lens (NA = 1.10, Olympus, Japan) was dipped into the culture medium to record the cell spectra. A continuous-wave background-free electronically tuned Ti:sapphire laser (CW-BF-ETL; Mega Opto, Japan) provided an excitation beam at 785 nm. The laser power was typically set to 30 mW during sampling. The exposure time was 90 s (30 s × 3 times). The microscope was equipped with a 60× water-immersion objective lens (NA = 1.10, Olympus, Japan), and a Raman polychromator, which has a grating (600 l/mm, 750 nm-blazed) and a Peltier-cooled CCD detector (DU-401-BR-DD, Andor Technology, Ireland). The spectral resolution was 5 cm^{-1}. This instrument was easy to focus on the sample and was used to record as many spectra as possible within a short period. The analyses were performed at 12, 24, and 48 h after addition of the virus to the cells. The experiments were repeated 5–20 times, and all the data were analyzed together.

The other Raman system was constructed in-house and involved an inverted fluorescence microscope. It was utilized for time-lapse experiments because it could keep cells for more than 24 h under the cultivation conditions. The excitation light at 785 nm was provided by a diode laser (Toptica, Germany). The laser power was typically set to 50 mW during sampling. The exposure time was 90 s (30 s × 3 times). The microscope was equipped with a 60× water immersion objective lens (NA = 1.10, Olympus, Japan), a Raman polychromator equipped with a grating (600 l/mm, 750 nm-blazed; Photon Design, Japan) and a Peltier-cooled CCD detector (DU-401-BR-DD, Andor Technology, Ireland). Given that the incubator has two places to set dishes (with control and virus-infected cells), the control and experimental dishes were maintained under the same stable conditions during the analysis. The time-lapse analysis was repeated three times, and the results were very similar.

To acquire the spectra, the laser was focused onto the nuclei of cells. The spectra were recorded in randomly selected cells in each dish. The spectrum of each cell was processed by background subtraction and 6th polynomial fitting to remove the artifacts caused by the culture medium and by the dish window. The intensities of the spectra were normalized to the band at 1004 cm^{-1}, assigned to phenylalanine residues. The spectra were also normalized to a band at 1440 cm^{-1}, assigned to a CH deformation mode, to confirm the results of multivariate analysis. The results obtained for the datasets normalized to the 1440 cm^{-1} band were always similar to those obtained for the datasets normalized to the 1004 cm^{-1} band. This finding suggested that the normalization procedures were valid. Multivariate-analysis software, Unscrambler (CAMO, Norway), was used for principal component analysis (PCA) and partial least square regression discriminant analysis (PLSR-DA). For the PLSR-DA, a dependent variable, –1 or 1, was included in the dataset to classify each dataset.

RESULTS AND DISCUSSION

The AdC viruses are recombinant adenoviruses capable of invading human cells by similar mechanisms. Given that AdC lacks the E1 gene, it cannot replicate in a normal human cell. However, it is able to do so in a HEK293 cell that has the E1 gene after transfection. E1 protein regulates the E2 gene, which encodes a DNA polymerase for replication of the viral genome. Figure 1 depicts immunostaining images of HEK293 cells infected with virus AdC (panels a–e). The antibody to the E2 polypeptide was applied to staining. In our previous paper, nuclei of virus-infected cells at 24 h showed strong fluorescence.1 In contrast, the entire cell body showed fluorescence in the present study because methanol staining here destroyed the nuclear membrane. Since the samples at 0

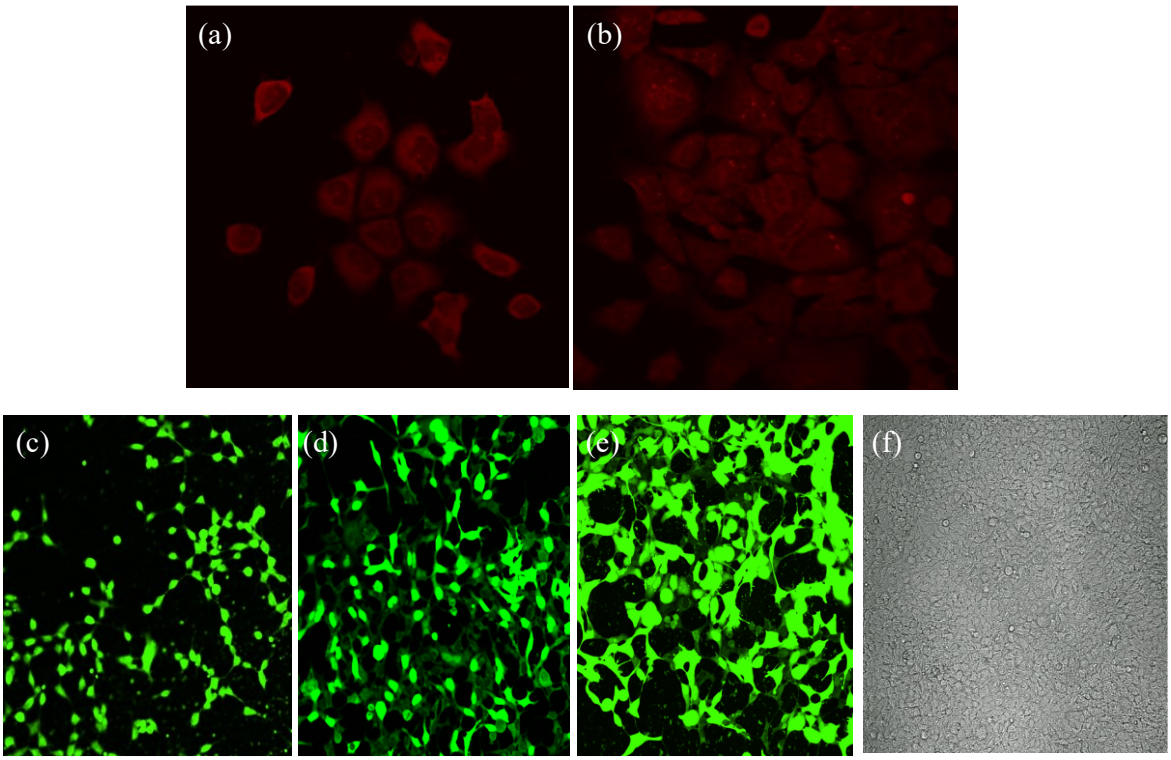

Fig. 1 Immunostaining images of HEK293 cells infected with the AdC virus, observed at (a) 0 h, (b) 3 h, (c) 12 h, (d) 24 h, and (e) 48 h after addition of the virus to the culture medium, and a bright-field image is also shown in (f). The cells were stained with a secondary antibody with (a and b) Alexa Fluor 546 dye and that with (c–e) FITC dye.

and 3 h labeled with the secondary antibody with FITC had showed no signal at the first experiment, they were, then, labeled with the secondary antibody with Alexa which has stronger fluorescent signal. (The filter set and light source were suitable for Alexa dye in our confocal fluorescent microscope.) Their images are depicted in Fig. 1(a and b). They similarly show only faint signals in the images, which are, however, due to nonspecific adsorption, indicating absence of the E2 polypeptide at 3 h after the infection. In contrast, the image at 12 h (Fig. 1(c)) already indicated the presence of the E2 polypeptide, suggesting that the E2 gene was transferred into the nucleus quickly after the virus invasion. The image in Fig. 1(c) shows that ~40% of the cells expressed the E2 polypeptide at 12 h, and the infection rate was almost 60–85% for the cells at 24 (d) and 48 h (e). This finding indicates that the rate of infection was high but not in all cells, and the

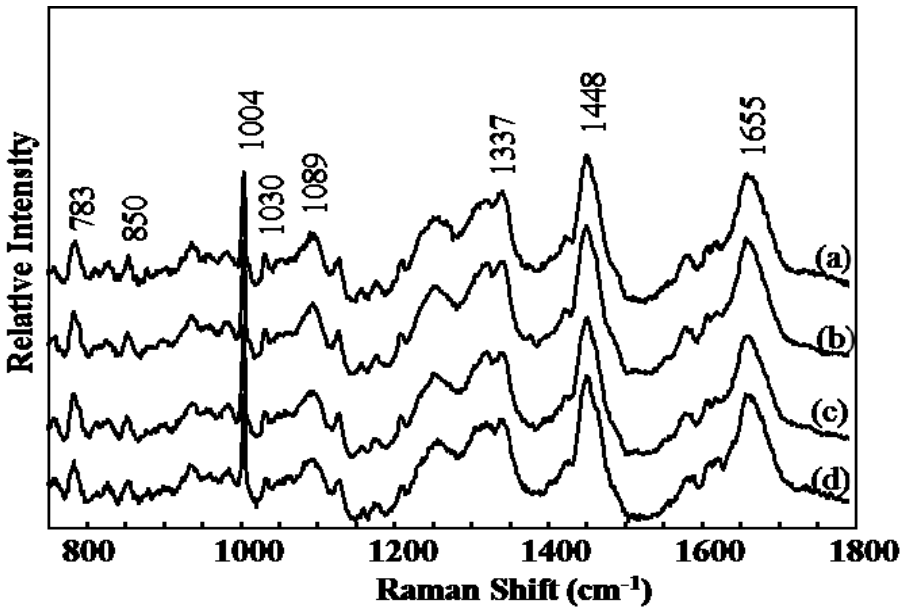

Fig. 2 Averaged Raman spectra of HEK293 cells (a and b) infected with the AdC virus or (c and d) not infected with the virus obtained at 12 and 24 h after addition of the virus, respectively.

concentration of the E2 polypeptide was low in the sample at 12 h and continuously increased within the cell for up to 48 h.

The averaged Raman spectra of the cells with AdC (a and b) and without the virus (c and d), acquired at 12 and 24 h, are presented in Fig. 2. The spectra are so close to each other that it is difficult to find a difference. Bands at 1655 and 1448 cm^{-1} were assigned to amide I and CH bending modes of proteins. A sharp band at 1004 cm^{-1} and a minor band at 1030 cm^{-1} were attributed to phenylalanine residues in the proteins. Smaller features at 1337, 1089 and 783 cm^{-1} attribute to adenine, PO_2^- symmetric stretch, and OPO symmetric stretch modes of DNA.[14,15] The observed spectra are similar to those reported in my previous paper.[1] Analyses were carried out at 3, 6, 9, 12, 18, and 24 h after the virus injection under the stable cultivation conditions. It took 2-3 min. for focusing on the nucleus and acquisition of the spectrum at each measuring site. To keep the synchronism in the dataset, the sample measurement was finished in 40 min. at each dataset. Therefore,

each dataset has relatively small number, 10-15, of spectra. PCA score plots for (A) PC1 and PC2 and (B) their PC2 loading plots for the datasets of control cells (○) and AdC virus-infected cells (◇). Results for datasets recorded at (a) 3 h, (b) 6 h, (c) 9 h, (d) 12 h, (e) 18 h, and (f) 24 h after addition of the virus. The PCA score plots of the datasets acquired at 3 h (a), 9 h (c), and 12 h (d) are depicted in Fig. 3A. (Those of the datasets recorded at 6, 18, and 24 h are shown in Fig. 5). The score plot at 3 h (a) suggests that the Raman

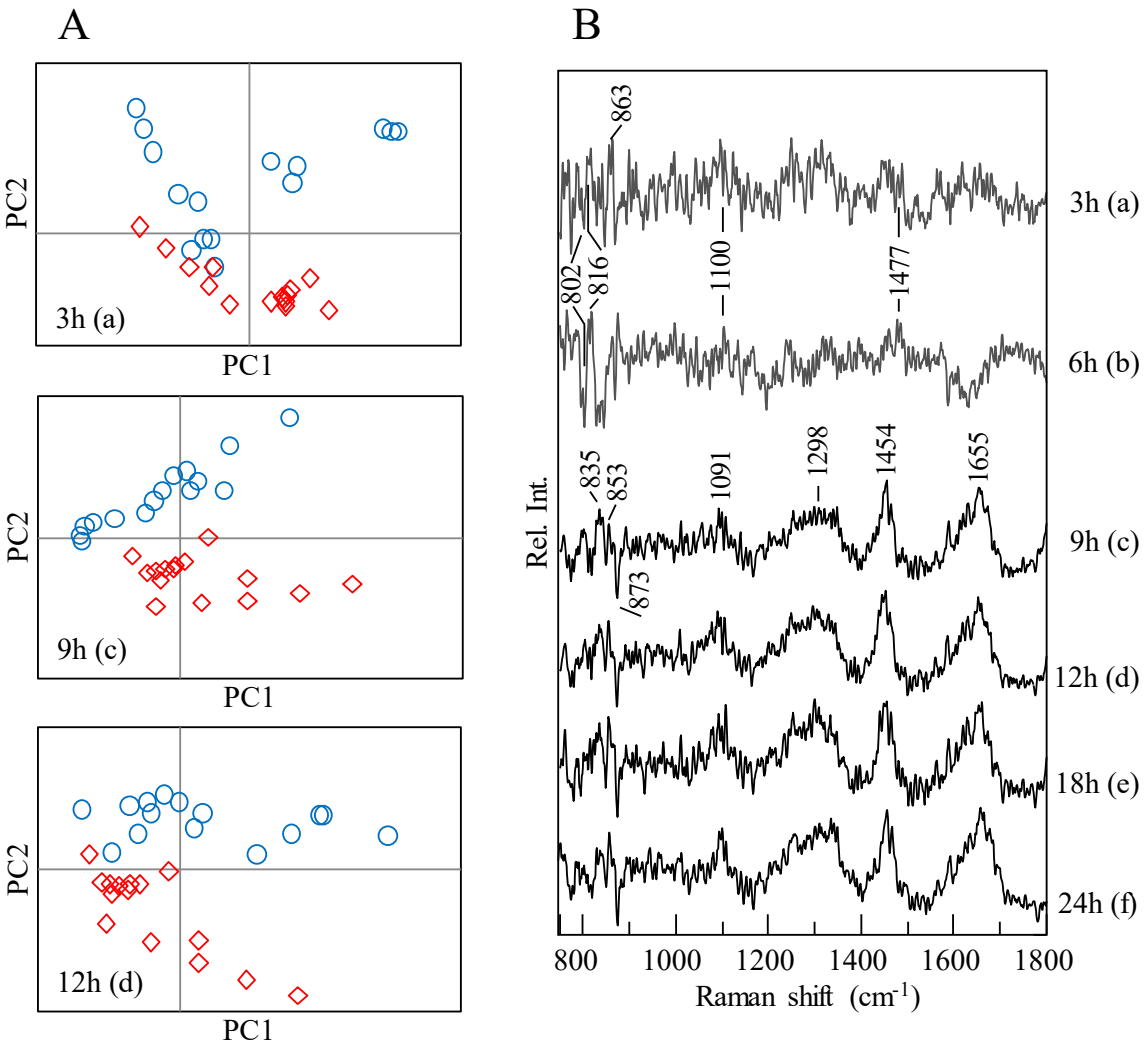

Figure 3 shows PCA analysis results for the datasets obtained in the time-lapse analysis of AdC-infected and control cells. I employed the Raman system with the inverted microscope, and spectra were repeatedly and alternately acquired from two culture dishes containing the infected and control cells placed in the CO_2 incubator on the microscope stage.

analysis already detected the virus infection at 3 h. The dispersion of data groups, however, overlaps, indicating that the virus invasion process is still under way in several cells. The score plot of the dataset recorded at 6 h (Fig. 5) also shows an overlap of the two groups. The score plots at 9 and 12 h revealed that the datasets of virus-infected cells are well discriminated from the datasets of uninfected control cells. Because it seemed that principal component (PC) 2 made a strong contribution to separation of these two data groups, the loading plot of PC2 represents the major difference in the spectra between the cells with and without virus infection. A similar tendency was observed for other data groups acquired at 6 and 18 h, but PC1 made an equally large contribution in comparison with PC2 for separation of the two data groups in the score plot at 24 h. (Fig. 5)

The loading plots of PC2 for datasets recorded at 3 h (a), 6 h (b), 9 h (c), 12 h (d), 18 h (e), and 24 h (f) are presented in Fig. 3B. At a glance, a remarkable difference is noticeable between the loading plots at 6 and 9 h. These data indicate that the reaction of the infected cell changed after 6 h. According to the spectral features in the loading plot at 3 and 6 h, the spectral difference between AdC-infected and control cells seems to be attributable to composition changes in DNA and RNA. DNA has a strong and broad band near 790 cm^{-1} and broad-shoulder bands near 830 cm^{-1}, which consist of overlapping small bands. RNA has a band near 783 cm^{-1} and a similar shoulder band. DNA also has strong bands near 1092 and 1488 cm^{-1}.

I assumed that the narrow sharp bands in positive and negative directions between 800 and 870 cm^{-1} in the loading plot at 3 and 6 h were generated by a wavenumber shift of the small bands constituting the broad bands derived from DNA and RNA. Small bands at 1100 and 1477 cm^{-1} are also assignable to DNA. The results agree with that of immunostaining observation in Fig. 1. In contrast, the loading plot of PC2 for 9-h (c), 12-h

(d), 18-h (e), and 24-h datasets (f) shows protein-like features. This result indicates that the composition of protein species suddenly changed and/or phenylalanine concentration increased in the nucleus of the virus-infected cells. (This is because a band of phenylalanine serves for intensity correction.) This finding suggests that transcription was activated, and the main process for translation of early proteins was moved out of the nucleus.

According to the time-lapse data, I hypothesized that there are two major postinfection reactions inside the cell after entry of the virus. One is the response of the cell itself (Rsp A). The reaction of the cell is partly known and includes antigen presentation and upregulation of lysosomes.[16] I assumed that this kind of reaction proceeds quickly after addition of the virus and is maintained consistently thereafter because the reaction must be faster than virus propagation to protect cells from the viral invasion. The other is production of early viral polypeptides and proteins to assemble viral particles (Rsp B). This kind of reaction proceeds gradually because the replication of DNA and synthesis of proteins consume a large amount of energy and materials. If these two reactions occurred during the virus infection process in cells, the effect of Rsp A would emerge several hours earlier than that of Rsp B. The Rsp A reaction at an early time point is probably difficult to detect by conventional methods because it does not involve production of proteins or nucleic acid replication in the first several hours. Because the cell must immediately react to the virus invasion, the reaction may activate certain functions and can result in localized molecular composition changes. The Rsp B reaction can be observed by conventional methods, as depicted in the fluorescent images in Fig. 1.

To analyze the origin of spectral changes in detail and to improve the reliability of the analysis, it is necessary to increase the number of data points in the datasets. The

number of data points was relatively small in my previous study.[1] The time-lapse analysis is a time-consuming process, and it is not possible to increase the number of data points within the limited period. There is another problem: background subtraction in the spectral processing for the time-lapse experiments. Because there was no time to acquire the background spectrum after the recording of each dataset, background spectra of the medium and dish were collected after the time-lapse examination. The same background data were shared to process all the data obtained in one experiment. Strictly speaking, this procedure should normally be avoided because there are differences in consumption and secretion of materials in a culture medium between the control and infected cells.[17] Therefore, I could not rule out that the present time-lapse data may be affected by the background spectra. Hence, I repeated the whole experiment many times to collect as much data as possible. In these experiments, the Raman system with an upright microscope was used, and the samples were prepared in a conventional CO_2 incubator. With the upright microscope, it was easy to find a target cell, but the water immersion objective lens that was inserted into the culture dish may cause contamination of the cell culture. The background measurements were carried out in every culture dish and were discarded after each Raman spectroscopy session. To keep uniformity of data and to minimize the time-dependent changes, the analysis was carried out only within 1 h in each culture dish where only 10–15 cells were analyzed. For technical reasons, it was difficult to conduct measurements earlier than 12 h after the infection. I obtained several dozen sample spectra as well as background spectra in the experiments independently repeated via the same procedure for further analysis. The datasets were subjected to PCA at first. In the PCA results of time-lapse spectra (Fig. 3), the spectral alterations due to virus infection were seen in the earliest components such as PC1 and PC2, which reflect the largest dispersion

in the datasets. In contrast, PCs from 1 to 7 yielded no remarkable categorization among these datasets, suggesting that they reflect spectral changes caused by cell conditions, such as slight differences due to cultivation conditions among the repeated experiments as well as inherent activities. I assumed that there were large irregular variations that were not related to the virus infection in this large set of data. The cell and virus are sensitive to alterations in the experimental conditions, such as concentrations of ingredients in the culture medium and conditions of storage, which technically cannot be eliminated. When the spectral changes due to the viral infection are smaller than that due to those irregular variations, it is difficult to find them in the earlier components in PCA. Hence, PLSR-DA was applied to extract variations that strongly correlated with the independent variable.[18] In the PLSR-DA, two datasets were analyzed together, where "−1" and "1" are tags for the

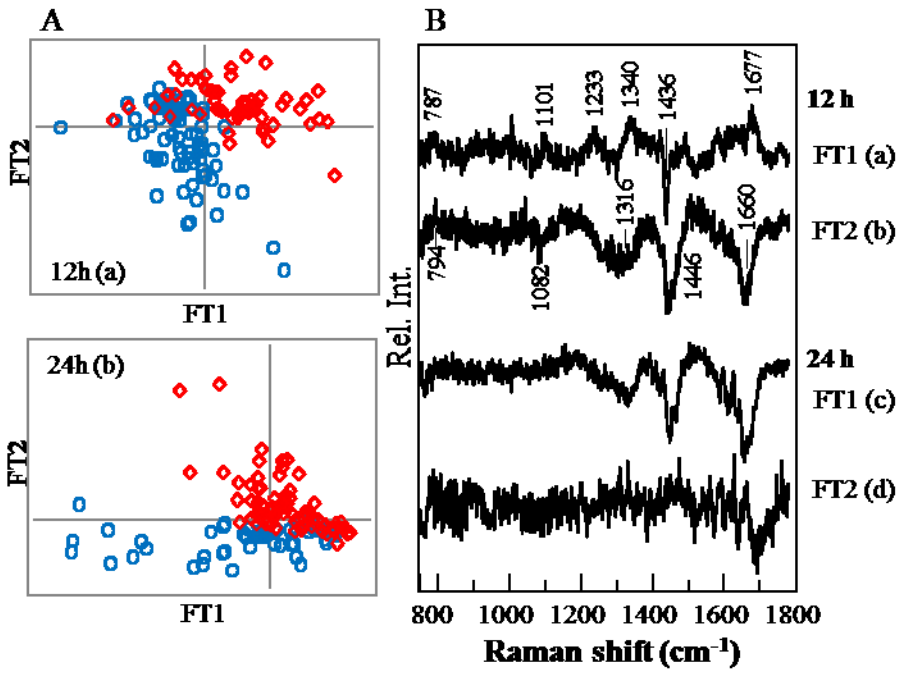

Fig. 4 PLSR-DA results obtained for control cells (○) and AdC virus-infected cells (◊). (A) Score plots for FT1 and FT2 calculated from the datasets obtained at 12 h (a, control: n ¼ 73; AdC: n ¼ 59) and 24 h (b, control: n ¼ 48; AdC: n ¼ 78) after addition of the virus to the cells. (B) Loading plots of (a) FT1 and (b) FT2 for the datasets acquired at 12 h, and (c) FT1 and (d) FT2 for the datasets recorded at 24 h.

independent variables. Therefore, a factor (FT) obtained by PLSR-DA was selected to make the dispersions of the two data groups distant, thus representing a characteristic difference between these data groups.

Score plots for FT1 and FT2 are depicted in Fig. 4A for the datasets of control cells and AdC-infected cells analyzed at 12 h (a) and 24 h (b) after addition of the virus. The dispersion in the dataset of the cells with a virus partly overlaps with that of the control cells. Several spectra of the infected cells are present in the control group, suggesting that the nonspecific spectral variance was quite strong and/or some cells were not infected by the virus yet as suggested by the immunostaining. The PLSR-DA model was validated by the one-leave-out cross-validation method. The correlation coefficient values (R^2) of the PLSR-DA models built for four factors were 0.842 and 0.665 for validation results of datasets acquired at 12 and 24 h, respectively. Loading plots of FT1 and FT2 for the models of 12-h and 24-h datasets are shown in Fig. 4B. The loading plots of FT2 for the

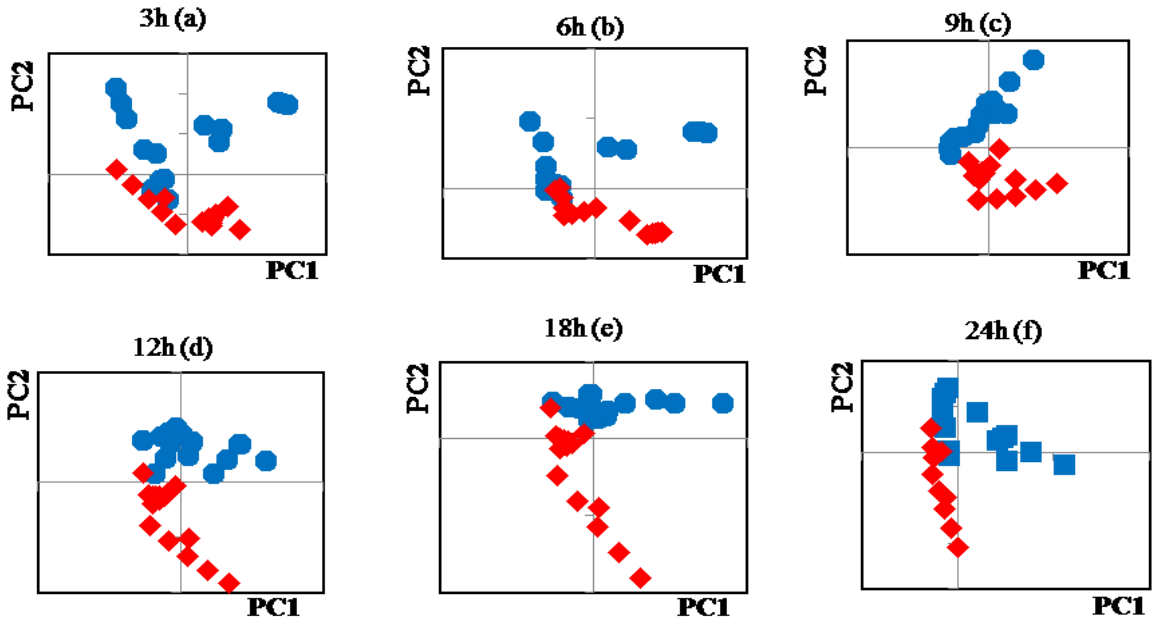

Fig. 5 The PCA score plots for PC1 and PC2 for the datasets of control cells (blue, circle) and AdC virus infected cells (red, diamond), recorded at (a) 3 h, (b) 6 h, (c) 9 h, (d) 12 h, (e) 18 h, and (f) 24 h after addition of the virus.

12-h dataset (b) and of FT1 for the 24-h dataset (c) look like that of PC2 (Fig. 3B (d)) in the time-lapse experiment in the higher-frequency region. The positive and negative direction are opposite because the direction of distribution in FT2 is opposite in the score plots (Figs. 3A (d) and 4A (a)). Bands at 1660 and 1436 cm^{-1} and broad features near 1340 cm^{-1} can be attributed to a protein. The negative direction of these bands indicates downregulation of proteins relative to the phenylalanine concentration, or the uptake of phenylalanine into the nucleus, because of the virus infection. However, the spectral features are slightly different in the low-frequency region. Bands at 787 and 794 cm^{-1} may be assigned to differential bands between DNA and RNA molecules. In case of plants, the response to pathogens would be accompanied by biosynthesis of aromatic compounds involving the conversion of phenylalanine.[19] However, any cellular response involving phenylalanine has not been reported for mammal cells, as far as we know. The present results suggest that Raman spectroscopy can detect virus infection in a live cell in vitro, even in its dormant state or during slow replication. This approach has advantages over the conventional methods, which require expression of viral genes.

Conclusion

Raman spectroscopy can detect the infection with adenovirus in a single live human cell without staining or labeling within only 3 h after addition of the virus to the culture medium. The analysis with a large number of datasets confirms that a HEK293 cell shows specific reactions to the virus infection. The present results suggest that there are two kinds of reactions taking place in the cell under the influence of virus infection. The first kind occurs instantly after the virus invasion. The second kind of reaction seems to represent

viral gene expression and replication of the virus particles. It seems to include uptake of phenylalanine into the nucleus and/or excess protein production.

REFERENCES

1. K. Moor, K. Ohtani, D. Myrzakozha, *et al.*, "Noninvasive and label–free determinstion of viruscells by Raman spectroscopy," *J. Biomed. Opt.* **19**(6), 067003-067008 (2014).
2. Salman, E Shufan, L Zeiri, *et al.*, "Characterization and detection of Vero cells infected with Herpes Simplex Virus type 1 using Raman spectroscopy and advanced statistical," *Methods* **68**, 364–370 (2014).
3. G. Glockzin, K. Mantwill, K. Jurchott, *et al.*, "Characterization of the Recombinant Adenovirus Vector AdYB-1: Implications for Oncolytic Vector Development," *J. Virol*. **80**, 3904-3911 (2006).
4. C. Silva, A. P. Teixeira, P. M. Alves, "Impact of Adenovirus infection in host cell metabolism evaluated by ^{1}H-NMR spectroscopy," *J. Biotech*. **231**, 16-23 (2016).
5. D. Cialla, T. Deckert-Gaudig, C. Budich, *et al.*, "Raman to the limit: tip-enhanced Raman spectroscopic investigations of a single tobacco mosaic virus," *J. Raman Spectrosc.* **40**, 240–243 (2009).
6. J. Lim, J. Nam, S. Yang, *et al.*, "Identification of newly emerging influenza viruses by surface-enhanced Raman spectroscopy," *Anal. Chem.* **87**, 11652−11659 (2015).
7. V. Hoang., R. A. Tripp., P. Rota *et al.*, "Identification of individual genotypes of measles virus using surface enhanced Raman spectroscopy," *J. Analyst* **135**, 3103-3109 (2010).
8. K. Hamada, K. Fujita, I. N. Smith, *et al.*, "Raman microscopy for dynamic molecular imaging of living cells*," J. Biomed. Opt*. **13**, 044027-044031 (2008).

9. G. J. Puppels, F. F. M. de Mul, C. Otto, *et al.*, "Studying single living cells and chromosomes by confocal Raman microspectroscopy," *Nature* **347**, 301–303 (1990).

10. W. Schie, T. Huser, "Methods and application of Raman microscopy to single-cell analysis," *J. Appl. Spectroscopy* **67**, 813-828 (2013).

11. J. R. Notingher, S. Jones, I. Verrier, *et al.*, "Application of FTIR and Raman spectroscopy to characterization of bioactive materials and living cells," *Spectroscopy* **17**, 275-288 (2003).

12. K. Hartmann, B. M. Putsche, T. Bocklitz, *et al.*, "A study of Docetaxel–induced effects in MCF-7 cells by means Raman microspectroscopy," *J. Anal. Bioanal. Chem*. **403**, 745-753 (2012).

13. K. Ohtani, A. Tsujimoto, M. Ikeda, *et al.*, "Regulation of cell growth-dependent expression of mammalian CDC6 gene by the cell cycle transcription factor E2F", *J. Oncogene* **17**, 1777-1785 (1998).

14. S. C. Erfurth, E. J. Kiser, W. L. Peticolas, "Determination of the backbone structure of nucleic acids and nucleic acid oligomers by laser Raman scattering," *Proc. Nat. Acad. Sci. USA* **69**, 938-941 (1972).

15. J. M. Benevides, G. J. Thomas Jr., "Characterization of DNA structures by Raman spectroscopy: high-salt and low-salt forms of double helical poly(dG-dC) in H_2O and D_2O solutions and application to B, Z and A-DNA," *Nucleic Acids Res.* **11**, 5747–5761 (1983).

16. J. E. Teigler, J. C. Kagan, D. H. Barouch, "Late endosomal trafficking of alternative serotype adenovirus vaccine vectors augments antiviral innate immunity," *J. Virology* **88**, 10354-10363 (2014).

17. T. R. Shojaei, M. Tabatabaei, S. Shawky, M. A. M. Salleh, and D. Bald, “A review on emerging diagnostic assay for viral detection: the case of avian influenza virus,” *Mol. Biol. Rep.* **42**, 187–199 (2015).
18. K. A. Lê Cao, S. Boitard, P. Besse, “Sparse PLS discriminant analysis: biologically relevant feature selection and graphical displays for multiclass problems,” *BMC Bioinformatics* **12**, 2-16 (2011).
19. J. F. Bol, H. J. M. Linthorst, B. J. C. Cornelissen, “Plant pathogenesis-related proteins induced by virus infection,” *Annu, Rev. Phytopathol.* **28**, 113-38 (1990).

Chapter 3

Study on viral invasion of live human cells using electron microscopy and gas chromatography

ABSTRACT

Virus infection in a live cell was successfully detected using Raman spectroscopy but there was not enough information on the localization of the virus to reveal the origin of the spectral changes. In the present study, a virus-infected cell was investigated using gas chromatography (GC) and transmission electron microscopy (TEM). In contrast to the Raman analysis, the GC study clearly showed no changes in the lipid composition between the cells with and without virus. The TEM study strongly suggested that the viral particles were observed in the cell and there was severe damage to the structure of cellular organelles and the cytoskeleton, which ascribes to the Raman spectral changes in the protein compositions. Hence, these results agree with the results of the Raman studies.

INTRODUCTION

In the previous chapters, I suggested that the virus-infected cell showed molecular compositional changes. Although almost all cells should have invasion of the virus according to the experimental procedure, I have directly confirmed the virus in the cells by immunostaining of the *E2* protein. The purpose of the present chapter was to confirm virus invasion into the cell and obtain information of the cellular changes with direct and destructive techniques, such as transmission electron microscopy (TEM) and gas chromatography (GC).

Electron microscopy is fundamentally a strong tool for the detection of concealed viruses, aside from the limitation of the optical resolution in microscopy. TEM uses an accelerated beam of electrons, which passes through a very thin specimen to enable a scientist to observe features such as structure and morphology.[1-3] TEM can be used to observe particles at a much higher magnification and resolution than can be achieved with a light microscope because the wavelength of an electron is much shorter than that of a photon.[4] It also provides higher resolution images than a scanning electron microscope, which can only be used to scan and view the surface of a sample.[5] Virologists use TEM to determine the size of a virus and identify fine structures as criteria for classification. However, this technique does not always succeed in detecting agents for some diseases, such as hepatitis and gastroenteritis, because susceptible cell cultures are not available for virus isolation or because the virus cannot be cultured.[6] TEM requires very thin specimens that are semi-transparent to electrons, which means sample preparation takes time. However, the high resolution TEM image is helpful to directly observe the virus particle in the cell. According to W. Doerfler, the size of the adenovirus is estimated to be 70 to 100

nm in diameter.[7-8] I have succeeded in obtaining a TEM image of recombinant adenovirus in HEK293 cells.

In contrast, chromatography is a technique to analyze the molecular components in cells. Sample preparation is the most important step prior to GC determination of an analyte. There might be several processes within sample preparation that depend on the complexity of the sample.[9] More recently GC has been used for the detection and identification of bacteria.[10] There are also studies of extract certification of virus-inoculated dogs with infectious hepatitis.[11] I used GC to identify recombinant adenovirus virus infection in HEK293 cells. The major bands in the loading plots categorizing the datasets of control and virus-infected cells are found at 1677, 1436, 1340 and 1230 cm-1, which are assignable to features of both protein and lipid.[12] I assumed that they arose mostly from proteins since the relative intensities among the bands were similar to those of protein. Since it was difficult to identify the origin of the bands only from the Raman spectra, I employed the conventional techniques that are destructive but are able to directly identify the origin. According to the Raman analyses, protein reproduction started from 9 h after the adenovirus infection. The immunostaining technique suggested that the infected cells expressed the early protein, *E2*, which was abundant enough to detect 12 h after the infection using immune reactions. These data suggested that complete copies of adenovirus existed in the cell after 12 h, at least, although it would be very few because 12 h is a very early state of propagation. The TEM observation revealed my assumption that the virus particles were found in the cell after 12 h. The GC technique was employed for the direct analysis of lipid species. If the origin of the loading plots included changes in lipid components, it would also be detected in the GC analysis.

EXPERIMENTAL

a. Preparation of virus-infected cells

Human embryonic kidney epithelial (HEK293) cells were purchased from DS Pharma Biomedical (Japan). The HEK293 cells were cultured in high-glucose Dulbecco's Modified Eagle Medium (DMEM; WAKO, Japan) supplemented with 10% fetal bovine serum (FBS; Beit HAEMEK, LTD., Israel) and 100 IU/mL penicillin (WAKO, Japan). Adenovirus (Ad-CMV-control) stock was prepared according to reported methods.[13] The virus was stored at −80 °C until use. The viral titer used was 0.5×10^6 PFU/mL, and the multiplicity of infection (MOI) was 6 PFU/cell. The cells were maintained at 37 °C and 5% CO_2 in a humidified incubator for 12 and 24 h.

b. TEM observation

TEM is often used to verify the condition of cellular organelles and direct observation of virus within cells. I used a procedure to ensure the observation of virus as well as the cellular organelle.[11] The control and virus-infected cells were detached from the culture dishes with a scraper (Sigma-Aldrich), then centrifuged at 1000 rpm for 10 minutes to pellet the cells. The pellets were washed three times with (–) phosphate-buffered saline (PBS) by gentle pipetting and centrifuged again at 1000 rpm for five min. The cells in the pellet were fixed by immersion in 2.5% glutaraldehyde-0.05 M cacodylate buffer (pH 7.4) at 4 ^oC for 2 h. The fixed cells were washed with the same buffer, then postfixed in 1% OsO_4 for 2 h. The cells were dehydrated through a graded ethanol series (50, 70, 80, 90, 95, and 100%), and immersed in propylene. The specimens were dispersed and attached onto Cu grids (Nisshin ltd., Japan) for ultrathin sectioning with a thickness of 70-90 nm. The sliced samples were negatively stained with uranyl acetate and then stained with lead

citrate to ensure a high contrast in the TEM images. TEM was carried out with a JEM-1400 transmission electron microscope (JEOL Ltd, Tokyo, Japan) and 80 kV.

c. GC analysis

The GC analysis was performed using a GC system (Shimadzu, Japan) with a flame ionization detector (FID). I employed a capillary column (DB-FFAP, 30 m, 0.32 × 0.50 mm, Agilent, USA) at the temperature of 250 °C with methyl decanoate $C_{11}H_{22}O_2$ as an internal standard. The cell was destroyed and dissolved with pure methanol in combination with heat treatment. The fatty acids in the cell were released from the glycerol esters and were transformed into their sodium salts. The sodium salts of the fatty acids were transformed into methyl esters by the methylation process to increase the volatility of fatty acids for the GC analysis. The methyl esters of the fatty acids were extracted from the aqueous solution into an organic solvent, such as hexane. A diluted basic solution was added to the sample test tubes to remove any free fatty acids trapped in the organic solvent and the hexane solution of the fatty acids was directly inserted into the GC instrument for analysis.

RESULTS AND DISCUSSION

There were morphological changes observed in the virus-infected HEK293 cells. The shape of organelles changed consecutively with the time of infection. Figure 1 shows TEM images of the cell without (a; control) and with (b) virus 12 h after the infection. In the image of the healthy cell (Figure 1a) that consists of two images, a nucleus with nucleolus is depicted at the center of the image and is surrounded by cytoplasm. The cells were closely attached and the neighboring cell and its nucleus were observed. There were

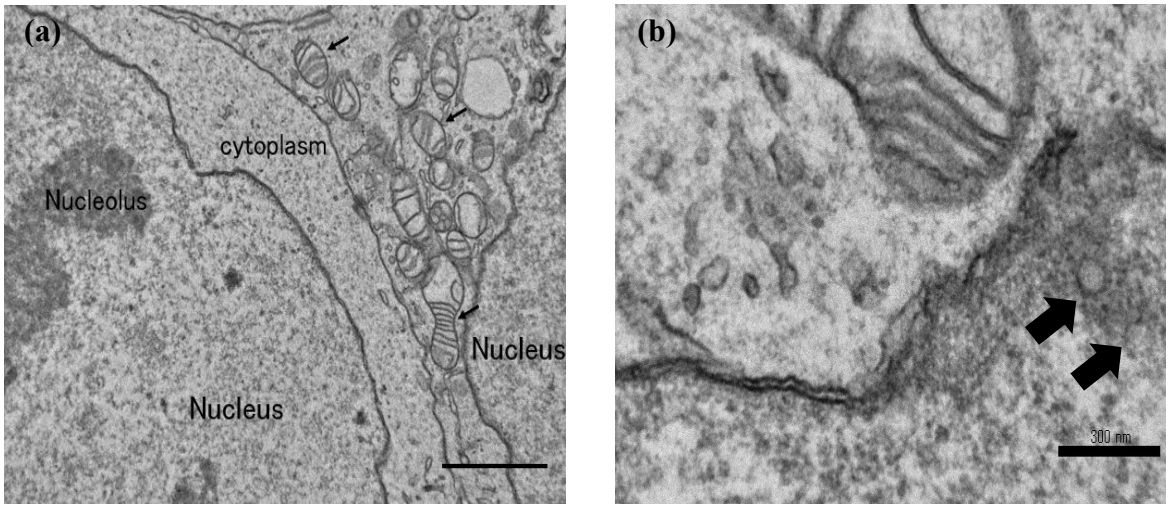

Fig. 1 TEM images of HEK293 cells without (a; control) and with (b) virus 12 h after infection. The scale bar is 1 μm in image (a) and is 300 nm in image (b).

many cross-sections of mitochondria observed in the neighboring cell. The cellular membrane was slightly thinner than the wall of the nucleus. The image of the virus-infected cell (Figure 1b) shows relatively unclear features. At 12 h after the infection, Raman analysis suggested the presence of viral DNA and duplicated adenovirus in the cytoplasm and that viral protein had been reproduced in the cell. Several black particles were observed in the cytoplasm that were not in the image of the control cell. Its size was estimated to be 90 nm, which was similar to the size of adenovirus reported by W. Doerfler.[7] Thus, I hypothesized that these particles of spherical shape were the duplicated adenovirus. The appearance of the present adenovirus looks like that of the particle virus (pV) reported by Merkow et al.[14] According to the theory of virus propagation, virus particles are produced in the cytoplasm. The viral DNA leaks from the lysosome in the cell and is carried into the nucleus. The early proteins are generated in the cytoplasm using viral DNA and they are imported into the nucleus. The early proteins quickly duplicate the

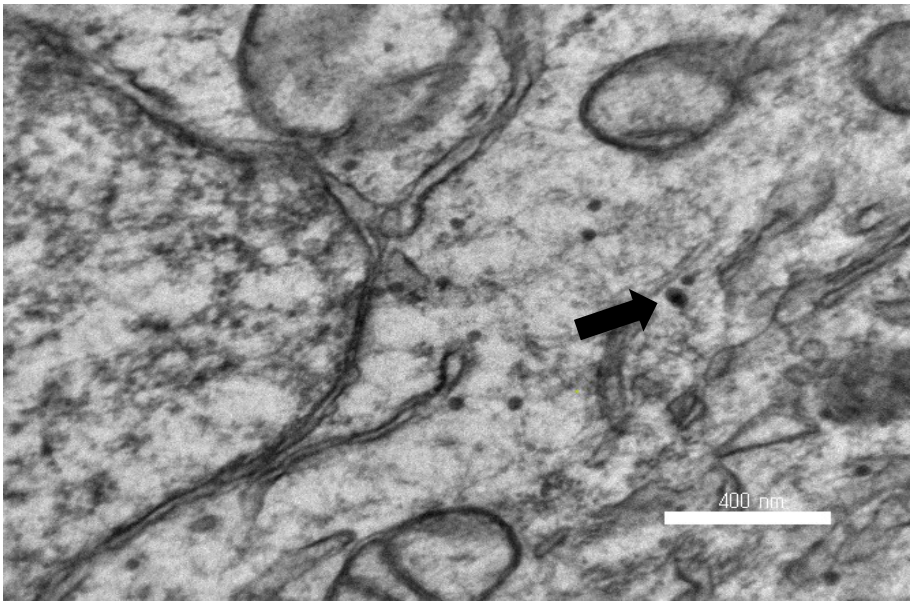

Fig. 2 TEM images of the virus-infected cell 24 h after infection the scale bar is 400 nm in image

viral DNA. The capsid proteins coded in the other part of the viral DNA are also translated and accumulate in the cytoplasm. When the capsid proteins encounter the viral DNA leaving the nucleus, a perfect copy of the adenovirus is built. In the TEM image of the cell 24 h after infection, the number of virus particles had increased in the cells (Fig. 2). Black spherical particles were found in the cytoplasm and were only observed in the virus-infected cells. These data strongly suggested that the black particles were the duplicated adenovirus in the cell. The image showed disintegration of the nuclear membrane, in that the thickness of the membrane became nonuniform. The cellular membrane was partly missing suggesting that it was destroyed during the staining process. These data suggested that the strength of the membranes in the cell was reduced by the adenovirus invasion. Since the energy of the cell was shared by the duplication of the virus, the cell was not able retain enough resources for cellular maintenance.

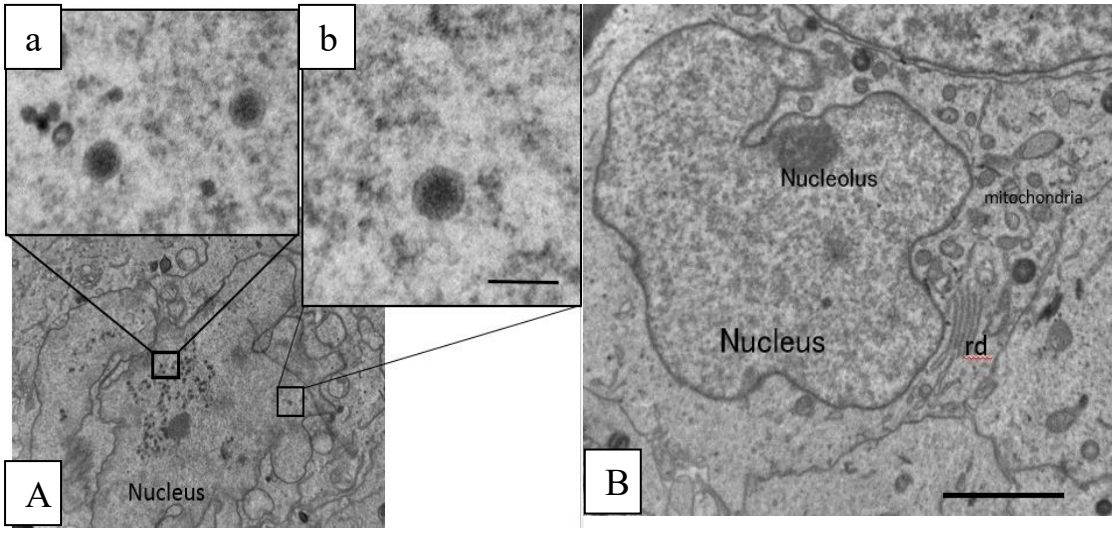

Fig. 3 TEM images of the cell with (A) and without (B; control) virus 48 h after infection. The images (a) and (b) are the enlargement of image (A). The scale bar is 1 μm in image (A), 100 nm in image (b). Image (B) is the counterpart image of the control cell. The scale bar is 1 μm.

Figure 3 depicts the TEM image of the cell 48 h after infection. It was estimated that the propagation of adenovirus had reached optimal conditions by this timepoint. The image indicated vacuolation of the cytoplasm and severe disintegration of the nuclear and cellular membranes, indicating that the cell was quite unhealthy. The black spherical particles were found in the nucleus and their size and shape were similar to those found in the cell cytoplasm at 12 and 24 h after infection, although the number of the particles had drastically increased.

Thus, I hypothesized that they were also duplicated adenovirus in the cell. In some cases of adenovirus propagation, the virus does not destroy the host cell but instead achieves a proviral state where it escapes the endocytic network, and tunes autophagy and microtubule trafficking to remain in a proviral state.[15] The visual observation (See Fig. 2B in Chapter 1) suggested that there were no morphological changes or changes in the survival rate of the cells at 48 h after infection. These data suggested that the adenovirus used in the present research had an ability to get across the membrane. My hypothesis was

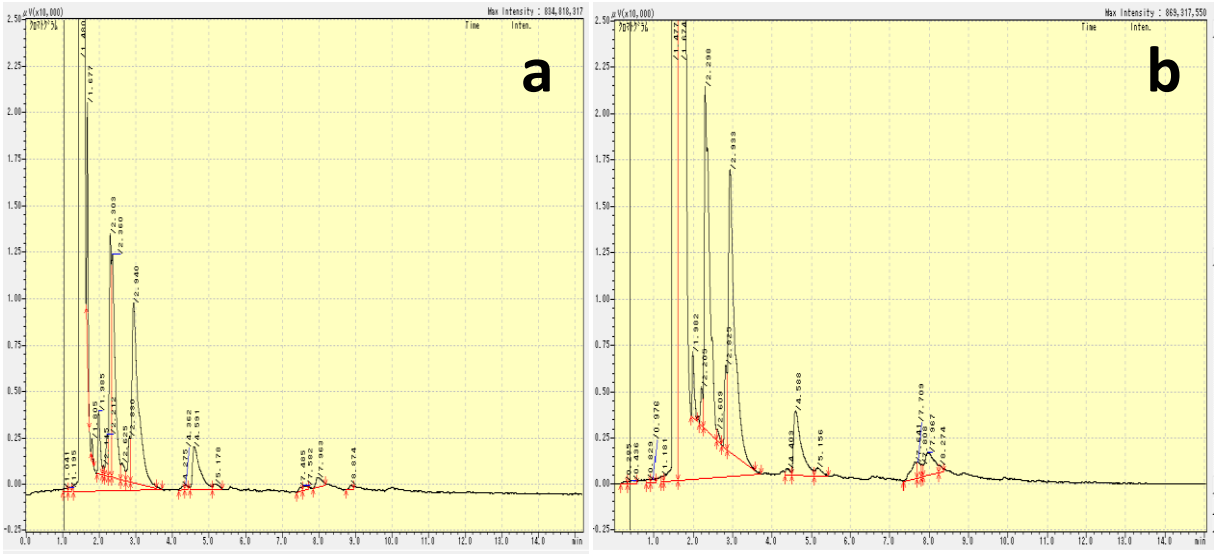

Fig. 4 GC spectra of the lipid species extracted from cells without (a; control) and with (b) virus 24 h after invasion.

that the viruses disrupted the organization of the cellular membrane to allow the duplicated virus to easily get across it. The virus observed in the nucleus would be those getting across the wrong membrane. The distribution of virus within both the cytoplasm and nucleus was also reported by Merkow et al.[12] The image is similar to that of lymphocytic virus.[16] The shape of the lymphocytic virus body was somewhat pentagonal and in this study the shape of virus's body was spherical, similar to the appearance of human immunodeficiency virus type 2.[17]

The next question was if the virus was able to change the composition of the lipid bilayer in the cell membrane. The Raman analysis suggested that spectral changes were observed in the virus-infected cells. According to the band assignments, the changes were mostly due to protein compositional changes but there was a possibility of a minor change in the lipid species. I used GC to determine the compositional changes in lipid species in the adenovirus-infected cells. The present method was able to measure the composition of fatty chains extracted from all lipid species in the cells. The GC spectra are shown in Fig. 4 for the control and virus-infected cells. The spectra showed no difference between the cells,

indicating that the adenovirus infection did not have any effect on the lipid composition. These data suggested that the adenovirus did not disturb any lipid production signaling pathways. This was reasonable because there was no particular gene included in the present recombinant adenovirus to interfere with any signaling pathway. In contrast, there were possibilities for chemical interference in protein production because viral propagation in the cell dominates other protein production. The present results revealed that the Raman spectral changes in the adenovirus-infected cell were due to compositional changes in proteins. The disorder in the membrane structures observed in the viral-infected cell was attributed to protein structural changes. There are protein structures under the cell and nuclear membranes to maintain the shape and strength of the membranes. The present observation suggested that the protein structure under the membranes was damaged by the reduction in normal protein production of the cell, resulting in the softening of the membranes. Since the structure under the nuclear envelope was damaged, the virus particles were found in the nucleus.

REFERENCES

1. G. J. Pupples, F.F. de Mul, C. Otto, J. Greve, M. Robert – Nicoud, D. J. Arndt – Jovin, and T. M. Jovin. “Studying single living cells and chromosomes by confocal Raman microscopy,” J. Nature 347, 301-303 (1990).
2. H. Malenovska. “Virus quantitation by transmission electron microscopy, TCID50, and the role of timing virus harvesting: A case study of three animal viruses” Journal of Virological Methods 191(2), 136-140(2013)
3. M. Sachsea I. Fernández de C. R. Tenoriob C. Riscob Chapter One - The viral replication organelles within cells studied by electron microscopy Advances in Virus Research 105, 1-33(2019)
4. Y. S. Bykov, M. Cortese, J. A. G. Briggs Ralf Bartenschlager “Correlative light and electron microscopy methods for the study of virus–cell interactions” FEBS Letters 590, 1877–1895(2016)
5. N. Uzunbajakava, A. Lenferink, Y. Kraan, E. Volokhina, G. Vrensen, J. Greve, and C. Otto, “ Nonresonant Confocal Raman Imaging of DNA and Protein Distribution in Apoptotic Cells,” J. Biophys. 84(6), 3968-3981(2003).
6. Rajan Arora, Georgi I. Petrov, Jian Liu, and Vladislav V. Yakovlev, “Improving sensitivity in nonlinear Raman microspectroscopy imaging and sensing,” J. Biomed. Opt. 16(2), 021114-021125 (2011).
7. Walter Doerfler, “Medical Microbiology. Adenoviruses” Chapter 67 (1996).
8. D. S.Ying L.Ying, L.Zong, Y. L.ShowAndre Lieber “Comparison of Adenoviruses From Species B, C, E, and F After Intravenous Delivery” Molecular Therapy 15(12):2146-53(2008).

9. K. Moor, K. Ohtani, D. Myrzakozha, O. Zhanserkenova, B. B. Andriana, H. Sato, “Noninvasive and label – free determinstion of viruscells by Raman spectroscopy,” J. Biomed. Opt. 19(6), 067003-067008(2014).
10. F. Falaki “Sample Preparation Techniques for Gas Chromatography,” DOI: 10.5772/intechopen.84259 (2019)
11. B. M. Mitruka1, M. Alexander, L. E. Carmichael “Gas Chromatography for Detection of Viral Infections,” Science REPORTS 160(3825), 309-31119(1968).
12. K. Ohtani, A. Tsujimoto, M. Ikeda and M. Nakamura, “Regulation of cell growth-dependent expression of mammalian CDC6 gene by the cell cycle transcription factor E2F,” *J. Oncogene* 17(14), 1777-1785 (1998).
13. J. J. Bozzola, and L. D. Russell, “Electron Microscopy Principles and Techniques for Biologists” Jones and Bartlett Publishers, Sudbury, MA. Chapter19 442-476 (1999).
14. . P. Merkow M. Slifkin “Oncogenic Adenoviruses. Biologic Parameters of Adenovirus Transformation1” Prog Tumor Res. Basel, Karger, 18, 166-198(1973).
15. J. W. Flatt and J. Sarah Butcher Adenovirus flow in host cell networks Open Biol. Feb; 9(2): 190012 (2019)
16. L. O. Zwillenberg, K. Wolf, “Ultrastructurae of Lymphocystis virus,” J. Virology, 2(4), 393-399(1968).
17. E. Palmer, M. Martin, C. Goldsmith, W. Switzer, “Ultrastructure of Human Immunodeficiency Virus Type 2,” J. Gen. Virol. 69, 1425-1429(1988).

GENERAL CONCLUSION

In the present research, I have successfully demonstrated that the Raman spectroscopy is able to detect the recombinant adenovirus invasion into the live HEK293 cell. Although the molecular change in the cell taking place after the viral invasion is slightly small comparing with the inherent cellular instability, the many repeated experiments revealed that the change due to the adenovirus infection is surely detectable by the present technique based on the Raman analysis. Since the technique does not utilize any specific gene or amino acid sequences, it is theoretically possible to apply any kinds of DNA viruses that are the same type of adenovirus. If I use a series of test cells that is usually used for the virus identification in the conventional method, it will be possible to detect and identify various human infectious viruses. The Raman analysis is so sensitive that the molecular change in the host cell is detected in only 3 h after the viral infection. It is not possible to recognize any morphological changes in the cell change up to 48 h after the virus infection. The immunostaining with an early protein, *E2*, is able to detect the virus infection at 12 h after the infection. According to the present knowledge for the mechanisms of viral infection, it is too early for the viral propagation activity to begin. When the adenovirus gets into the cell by endocytosis, it is transferred into lysosome and unpacked. The DNA of the virus sneaks out from the lysosome by the help of a capsid protein consisting of the envelope and transferred into the nucleus. I refer the above process as the first reaction. Then, RNAs coding early proteins are copied form the virus DNA, translated into the proteins and transferred back into the nucleus. I refer the following process as the second reaction. As confirmed by the *E2* immunostaining observation, the total process including the first and second reactions takes 8-12 h. The time-depending analysis suggests that the spectral difference to discriminate virus infected

group is the compositional changes in DNA and RNA at 3 and 6 h but it attributes to the changes in protein species from 9 h after the virus infection. It is reasonable for the viral infected cell to have the protein changes because the excess early proteins are accumulated in the nucleus in the second reaction. In contrast, the first reaction is very small because the one virus has only one DNA. It is not reasonable for Raman spectroscopy to detect the changes due to only 1 DNA in the cell. Consequently, I make an assumption that the cell is able to detect the virus invasion and makes defense reactions against the virus. When the cells detect the intruder, it activates signaling pathways immediately to translate to make reaction. It may be a reaction to pass a signal to the immune system, such as antigen presentation. It is, however, necessary to confirm with the additional research using different type of viruses and cells.

The direct observation with TEM revealed the virus particles in the infected cell. Besides, the TEM study suggests some additional reactions of the host cell. The membranes of the cell as well as organelle are disordered slightly in the virus infected cell at 12-48 h after the virus infection. The GC study revealed that there are no changes in the lipid species composition, suggesting that the instability of the membranes attribute to the disorder in the protein lining structures under the membrane. The present recombinant adenovirus does not code any toxic protein but is able to propagate in the HEK293 cell. It suggests that the cellular reaction is proper reaction for the adenovirus coded in the main genes to propagate.

In the present research, I have made a several new observations that may bring a new insight into the virus study. The present Raman analysis of the virus infected cell is the totally isolated observation technique for the virus study. There is no necessity to touch or treat the sample with virus. As it is discussed in General Introduction of the thesis, there

are new human infectious viruses found and some of them are highly lethal to human. If it is possible to make sampling of the virus from the field, the present technique is able to detect it, without patients and any risk of infection.

Further and more detailed study of the virus by Raman Spectroscopy may well answer the still interesting questions for scientists. When, exactly the transformation of normal cells by viral infection or other factors into the cancer cell occurs. If this issue is closed I think we will stand on a new era of scientific research favorable to all living world.

ACKNOWLEDGMENTS

I would like to thank, with my sincere gratitude first and foremost, my advisor Professor Hidetoshi Sato for invaluable and continuous support of my PhD study and research, for his patience, inspiration, and immense knowledge. His guidance helped me in all the time of research and writing of this thesis. I could not have imagined the better advisor to my PhD study.

I owe my deepest gratitude to Professor Kiyoshi Ohtani for his kind regards and supports in virus research and also I would like to big thank Professor Satoru Kato and his PhD student Tsubasa Miyoshi for help with Transmission Electron Microscopy. It gives me great pleasure in acknowledging the support and help of Dr. Bibin Bintang Andriana. And I appreciate with big gratitude to laboratory assistants of Kwansei Gakuin University especially to Chief experimental training teacher Sachiko Tominago. This thesis would have remained a dream had it not been for Yusuke Terada master student and co-author of my published paper. This assignment couldn't be completed without the efforts and cooperation our group members. My appreciation, to Akinori Taketani and Kasuke Hashimoto for their active participation and valuable suggestions.

I cannot find words to express my gratitude to Yoshida Scholarship Foundation which gave me the opportunity not only to gain invaluable knowledge but also to discover a wonderful Japan.

Last and not the least I would like thank my family, my parents Alexander Moor and Aliya Moor, my twin brother Kamil Moor for supporting me all my life and not letting me give up during my PhD study

LIST OF PUBLICATIONS

Journal Article

1. Moor K., Terada Y., Taketani A., Matsuyoshi H., Ohtani K., Sato H. Early detection of virus infection in live human cells using Raman Spectroscopy. *J. Biomedical Optics* **29**, 097001-1-7, September (2018).
2. Sergiienko S. A., Moor K., Gudun K., Elemesova Z., Bukasov R. Nanoparticle-nanoparticle vs nanoparticle-substrate hot spot contributions to SERS signal studying Raman labeled monomers, dimers and trimers. *J. Physical Chemistry Chemical Physics* **18**, 1-636. December (2016)
3. Moor K., Ohtani K., Myrzakozha, D., Zhanserkenova, O., Andriana, B.B., Sato, H. Noninvasive and label-free determination of virus infected cells by Raman spectroscopy, *J. Biomedical Optics* **19**, 67003-1-5, June (2014).
4. Sato H., Taketani A., Moor K., Hashimoto K., Meksiarun P., Ishigaki M., Maeda Y., Andriana B.B. Raman Spectroscopy in Studies on Live Cells and Tissues. *Advanced Science, Engineering and Medicine* **6**, 899-901. August (2014).
5. Alzahrani S., Sawa M., Hashimoto K., Moor K., Andriana B. B, Kato S., Yagura T., Hidetoshi S. Free Labeling Diagnostic for Biochemical Changing of Pancreatic Cancer Cell Treated by Caffeine. *Advanced Science, Engineering and Medicine* **6**, 889-891. August (2014).

Proceedings

1. Moor K., Ohtani K., Myrzakozha D., Zhanserkenova O., Andriana B.B., Sato, H. Analysis of virus infected cell by Raman spectroscopy and transmission electron microscopy. Proc. SPIE 8939 San Francisco, California, USA, (2014).

2. Moor K., Kitamura H., Hashimoto K., Sawa M., Andriana B.B., Ohtani K., Yagura T., Sato H. Study of virus by Raman spectroscopy. BiOS-SPIE, San Francisco, California, USA. 8587: 85871X-1 – 85871X-7 (2013).